

Chapter 2

The Delivery of tRNA to Cultured Mammalian Cells Mediated by Peptide Transduction Domains

Abstract

In vivo incorporation of unnatural amino acids using nonsense suppression is a powerful technique to study proteins. However, one challenge to the method is that the amount of unnatural protein that can be produced is directly limited by the amount of unnatural aminoacyl-tRNA presented to the cellular translation machinery. Therefore, the success of this technique depends heavily on the ability to deliver aminoacyl-tRNA, which is produced *in vitro*, into cells. Currently, the most commonly used system involves injection of a *Xenopus* oocyte. It is desirable to transfer the technology to a mammalian expression system, but because mammalian cells are so much smaller than oocytes, injection is not a practical delivery method, so other techniques must be utilized. An intriguing possibility is the use of protein transduction domains (PTDs), small peptides that greatly enhance the internalization of extracellular material. Several PTD-based approaches for tRNA delivery were attempted: covalent ligation of tRNA to a PTD, noncovalent complexation of tRNA and PTDs, and production of a fusion protein containing a PTD and a tRNA-binding domain. However, none of these methods was useful in delivering tRNA into mammalian cells in culture.

INTRODUCTION

Unnatural Amino Acid Incorporation by Nonsense Suppression

Proteins are the workhorses of the cell. This class of biological macromolecules is involved in essentially every process necessary to sustain life [1]. Given the incredible diversity of protein functions, it is remarkable that practically all proteins in all forms of life are built from a set of just twenty amino acids. Within each protein, specific residues play important roles, giving the protein the characteristics required to carry out its function [2]. Obtaining a detailed understanding of a protein's operation as a molecular machine depends heavily on the elucidation of its important residues and the roles that they perform.

A common method for studying proteins involves mutating particular residues to other amino acids and determining how the change affects protein function. This technique can provide a wealth of information about the involvement of the residues in intra- and intermolecular binding and recognition interactions as well as the catalytic mechanisms of enzymes. With the discovery of the genetic code, the site-specific mutation of one amino acid to another has become a straightforward process. However, conventional mutagenesis techniques are limited to the set of twenty natural amino acids, which provide a relatively narrow range of chemical functionalities.

To overcome this limitation, a technique for incorporating unnatural amino acids has been developed to expand the set of amino acids available for mutagenesis beyond the natural twenty [3]. A wide variety of amino acids, subtly or drastically different from the natural amino acids, have been site-specifically incorporated into proteins, which has

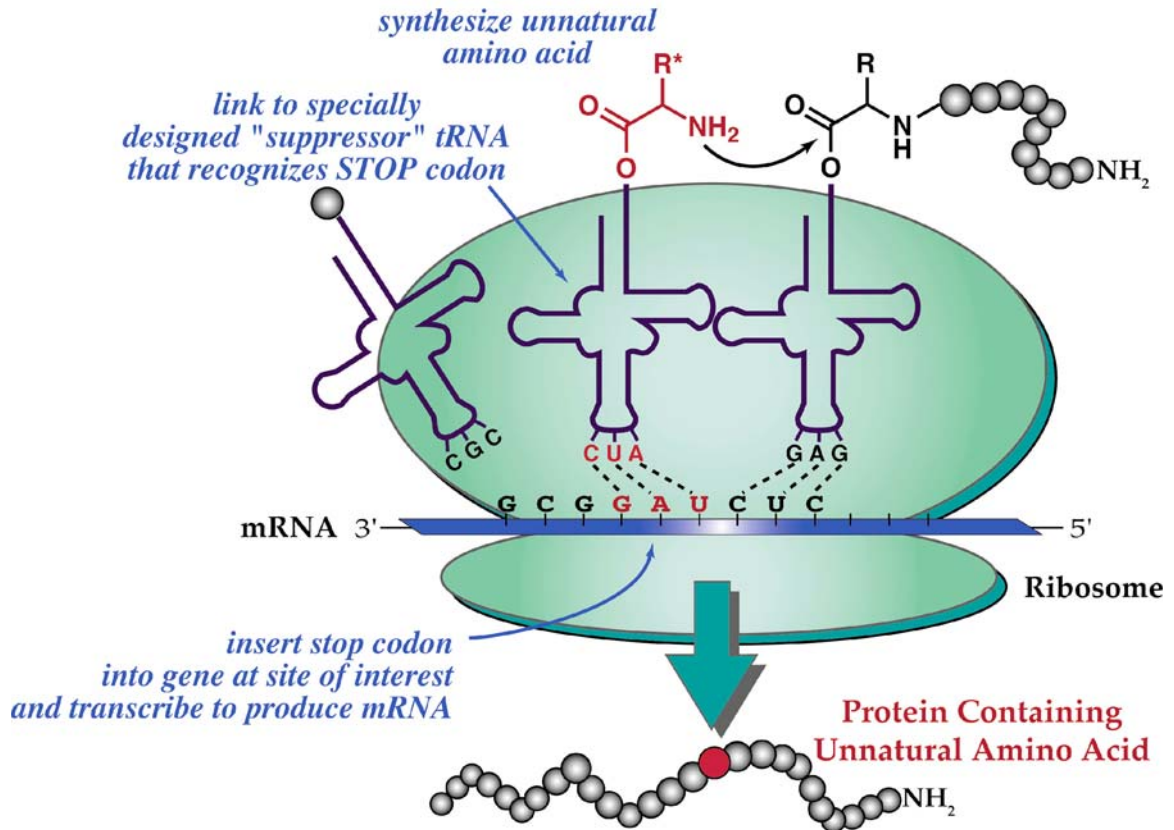


Fig. 2.1. The nonsense suppression method for unnatural amino acid incorporation.

opened the door to a whole world of new experiments. Proteins can be studied in much finer detail, and proteins with novel properties can be generated [4–8].

The technique takes advantage of the phenomenon known as nonsense suppression, in which a codon that ordinarily is noncoding is manipulated and used to incorporate a unique amino acid (fig. 2.1) [9, 10]. The site of interest within the gene is mutated to a stop codon, which normally signals for the termination of translation and has no cognate tRNA molecules. In addition, the desired unnatural amino acid is chemically ligated to a specially designed suppressor tRNA containing the stop anticodon. The mutated gene and the suppressor tRNA are presented to the cellular translational machinery, either *in vivo* or *in vitro*. The synthesis of the protein proceeds normally at

first, but when the machinery reaches the stop codon that has been inserted into the gene, instead of terminating translation, it binds the suppressor tRNA and appends the unnatural amino acid to the nascent polypeptide chain. The rest of the polypeptide is then synthesized normally, producing a full-length protein with the unnatural residue at the desired site.

An important challenge in the production of unnatural proteins by this method is the fact that the unnatural aminoacyl-tRNA is a stoichiometric reagent. Because the aminoacyl-tRNA is not regenerated, the number of proteins that can be produced is directly limited by the number of aminoacyl-tRNA molecules delivered to the system. Therefore, this technique hinges on the ability to deliver sufficient amounts of tRNA to the ribosomes. Until recently, the only *in vivo* expression system that could be used to generate and study unnatural proteins was the oocyte of *Xenopus laevis* [11, 12]. Its large size allows for easy tRNA delivery by injection through the membrane.

Although in many cases the *Xenopus* oocyte system works well, there are clear benefits to transferring this technology to a mammalian cell expression system. Many of the proteins that have been studied with unnatural amino acids are ion channels of mammalian origin. Several of these channels do not express well in oocytes, and it is likely that their expression could be improved in a more native environment. Furthermore, expression in mammalian cells will allow for studies on signaling pathways that are absent in oocytes. However, progress on developing a mammalian cell expression system for unnatural proteins has been slow, because mammalian cells (~10 μm in diameter) are so much smaller than oocytes (~1 mm in diameter), making it much more difficult to deliver enough tRNA to produce a detectable amount of protein.

Our lab has only recently developed the methodology for generating unnatural proteins in mammalian cells [13]. Electroporation was chosen from a number of transfection techniques as the most suitable method for delivering the mutated mRNA and suppressor tRNA to the cells. Although this technique works reasonably well, other methods should be explored to improve the delivery of tRNA, and as a result, produce more protein.

Protein Transduction Domains

An intriguing possibility is the use of protein transduction domains (PTDs) as delivery agents for tRNA. PTDs, also known as cell-permeable peptides or CPPs, are relatively short peptides, ranging from 7 to ~40 residues in length, that have the capability to cross through biological membranes [14–17]. At least twenty distinct sequences from natural proteins have been discovered to have PTD properties, and many derivatives of these have been developed. The best characterized include the PTDs from the Antennapedia homeoprotein from *Drosophila* (Antp or penetratin) [18] and the HIV-1 transactivator of transcription (Tat) [19].

Amazingly, the peptides can confer their translocation properties to other molecules. Conjugation or tight noncovalent association of PTDs to other molecules or molecular assemblies facilitates the delivery of the full cargo into the cytoplasm. The diverse range of the cargo that PTDs have delivered includes other peptides [20, 21], fluorophores and drugs [22, 23], full-length proteins [24–26], DNA and peptide nucleic acids [27–29], magnetic nanoparticles [30], and intact liposomes [31]. Thus, PTDs

Table 2.1. Primary sequences of selected PTDs.

PTD	Sequence^a
Antp	RQIKIWFQNRRMKWKK
Tat	YGRKKRRQRR
MPG ^b	Ac-GALFLGFLGAAGSTMGAWSQPKSKRKV-Cya

^a Basic residues are shown in blue to highlight their abundance. ^b MPG has an acetyl group (Ac) at its N-terminus and a cysteamide residue (Cya) at its C-terminus.

appear to act as nonspecific delivery agents, and the mechanism of the uptake of PTDs into cells has been an area of intense research.

Other than the fact that PTDs generally contain many basic and hydrophobic residues, they do not have any obvious sequence or structural similarity, as shown by the examples in table 2.1, which contains the sequences of the PTDs that were used in this study. Initial experiments indicated that PTDs were able to cross membranes rapidly in an energy-independent, receptor-independent, and nonendocytotic manner. However, more recent work has demonstrated that most of these assertions were based on artifactual results [32–36]. The current leading hypothesis on the translocation of PTDs involves tight, nonspecific binding of the PTD to the cell surface phospholipids and polysaccharides through electrostatic interactions, followed by endocytosis and release from the endosomes into the cytoplasm or nucleus. There is still debate on the precise details, however, and it is possible that in some cases, PTDs may actually traverse the membrane via a nonendocytotic mechanism [36–38].

PTDs are an attractive option for efficient delivery of unnatural aminoacyl-tRNA into mammalian cells. There are several PTD-based approaches for tRNA delivery: covalent ligation of a PTD to a tRNA molecule, the formation of large noncovalently associated PTD/tRNA complexes, and the generation of a fusion protein consisting of a

tRNA-binding domain linked to a PTD. There are no reports of tRNA delivery with PTDs in the literature, so all of these options were explored to determine which, if any, is the most viable method.

RESULTS AND DISCUSSION

Covalent Ligation

The most straightforward methodology for employing PTDs to transfect mammalian cells with tRNA involved forming covalently linked conjugates. Although this approach has not been previously reported for RNA delivery, covalently linked conjugates with DNA have been used several times [27, 28]. Conjugation requires the presence of reactive groups on both the PTD and the cargo molecule. As short peptides, PTDs can be easily generated by solid-phase synthesis, which allows for a wide variety of reactive groups to be appended to the peptide chain. Similarly, short oligonucleotides can be prepared by solid-phase techniques with an appropriate chemical group. Many peptide-DNA conjugates have been made by reacting the two molecules prepared in this manner [39]. To date, the largest DNA strand that has been conjugated to a PTD is 55 nucleotides in length [40]. However, for larger nucleic acids, such as plasmids, full-length mRNA transcripts, or tRNA molecules, solid-phase synthesis is inefficient and prohibitively expensive. It is much easier to generate them by biochemical means, but this method does not allow for the incorporation of any chemically reactive groups that could be used for conjugation. Consequently, there are very few strategies for the chemical modification of nucleic acids.

One possibility that was considered for modifying a biochemically produced tRNA transcript involved successive treatment of the tRNA with alkaline phosphatase, to remove the 5' phosphates, and polynucleotide kinase with ATP- γ -S, to append a thiophosphate to the 5' end of the tRNA [41]. If the thiophosphate has chemical properties similar to thiols, it will be capable of reacting with a maleimide group attached to a PTD.

The reaction of the thiophosphate-modified tRNA (tRNA-5'-S) with a PTD-maleimide was attempted, but was not successful in forming a covalent linkage between the two molecules [42]. There are at least two possible explanations for the failure of this reaction: (1) nonspecific association through electrostatic interactions of the highly negative tRNA and the positive PTDs prevented the reactive groups from coming into contact, or (2) thiophosphates are not very reactive towards maleimides at the concentrations used in our preparations.

Explanation (1) was previously explored and found to be unlikely, for several reasons. First, the formation of the conjugate was not enhanced by the presence of a high salt concentration in the buffer. Ionic screening of the interactions between the tRNA and PTD should have decreased the amount of nonspecific binding. Second, the use of Tat-4, a Tat analogue containing only 3 basic residues (instead of 7 on Antp, for example) did not improve the formation of the conjugate [42].

However, explanation (2) remained to be tested. Thiophosphates of mono- or dinucleotides at concentrations of ~ 10 mM have been shown to be at least modestly reactive towards maleimide reagents [43–45], but there is much less data for lower concentrations, such as those in the range of 1–10 μ M that can be produced for

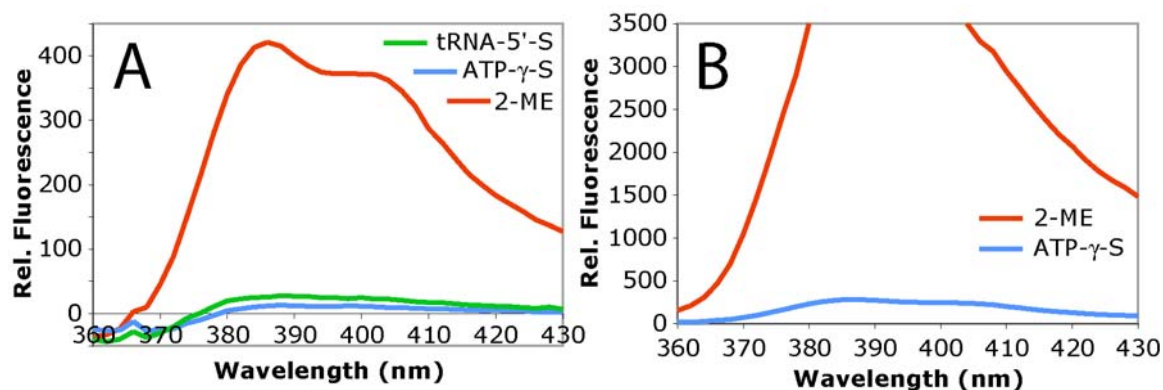


Fig. 2.2. Emission spectra showing the fluorescence of PM after reaction with various thiol or thiophosphate compounds, relative to the fluorescence of PM alone. *A*, 5 μM thiol/thiophosphate and 50 μM PM. At wavelengths less than 375 nm, there were strange peaks in the raw data, which seemed to be related to the plate itself. The fluorescence of the unreacted PM solution had an unusually large peak there, which caused the relative fluorescence curves shown here to dip below zero. Despite this, the peak PM fluorescence is obvious at 386 nm. *B*, 12.9 μM thiol/thiophosphate and 50 μM PM. The fluorescence of the 2-ME solution saturated the detector.

tRNA-5'-S. Therefore, the hypothesis that thiophosphates at low concentrations do not react efficiently with maleimides was explored by using N-(1-pyrenyl)maleimide (PM) as a probe molecule. PM is nonfluorescent unless a thiol or thiophosphate reacts with the maleimide moiety.

The reactivity of tRNA-5'-S with PM was measured by monitoring the PM fluorescence. 5 μM of tRNA-5'-S, ATP- γ -S, and 2-mercaptoethanol (2-ME) were incubated with 50 μM PM, and the fluorescence emission spectrum for each reaction mixture was obtained after 27 hours (fig. 2.2A). The 2-ME reacted very well with PM, but reaction of the thiophosphate compounds could not be detected.

The concentration of the thiol/thiophosphate compounds was increased to 12.9 μM , which is near to the highest practical concentration of tRNA-5'-S that can be produced by PNK treatment and dialysis. This experiment did not include tRNA-5'-S because there was not enough material to make such a highly concentrated solution. It is

clear there is some reactivity of the thiophosphate of ATP- γ -S with the PM (fig. 2.2B), but it is approximately an order of magnitude less than that of the thiol of 2-ME, which saturated the detector at this concentration.

Therefore, generating a 5'-thiophosphate by AP and PNK treatment of the tRNA failed to provide a reactive chemical handle for linkage to PTDs. This result, together with the fact that linking a PTD to any nucleic acid produced biochemically has never been reported in the literature, leads to the conclusion that the formation of a covalently linked PTD-tRNA conjugate is particularly difficult and is not a practical option for tRNA delivery.

Noncovalent Delivery Complexes

Because of the difficulty in preparing covalently linked PTD-tRNA conjugates, the method of tRNA delivery by noncovalent complexation with PTDs was explored. This method was used in the only report of RNA delivery with a PTD to date. Divita and co-workers used the 21-residue peptide MPG to transport plasmid DNA as well as mRNA into the nuclei of living cells [46]. Based on this work, MPG was chosen for study in our system.

MPG was prepared by solid-phase synthesis. HPLC and MS analysis indicated that the final product was very pure and had the desired mass (fig. 2.3).

Complexation of MPG with Nucleic Acids

The tryptophan fluorescence of MPG can be used to monitor its complexation with nucleic acids [47, 48]. Plasmid DNA binds MPG with a relatively high affinity,

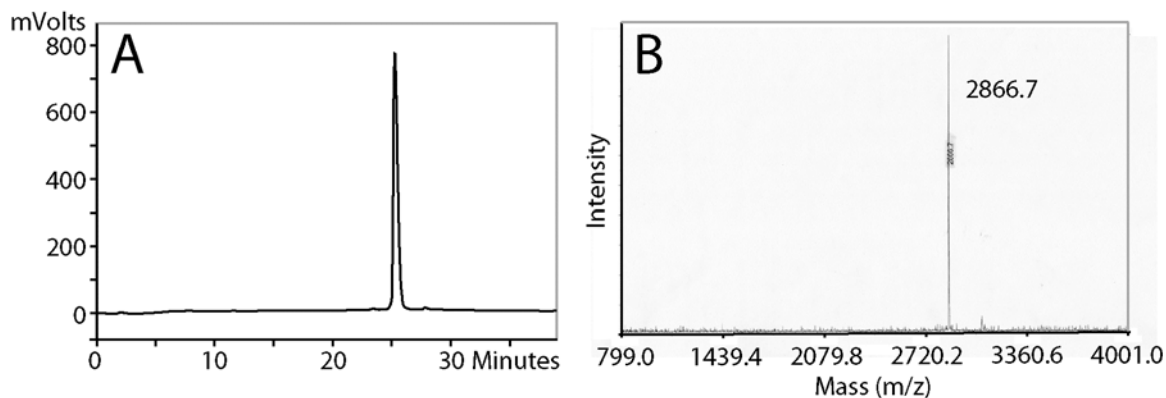


Fig. 2.3. HPLC trace (A) and MS (B) of MPG prepared by solid-phase synthesis, indicating the purity of the product. The MS peak was expected to be 2867.4, indicating that the desired product was synthesized.

quenching the fluorescence of MPG by up to 30%. In experiments with 10 μM MPG, only 0.5 nM DNA was required for 15% quenching (half of the full reduction of fluorescence), and 2 nM DNA was sufficient for maximal quenching. As a first step in our work with MPG, we attempted to reproduce this work.

Two different plasmids—pTAT (2955 bp) and pCS2 containing an EGFP gene (~4800 bp)—were used. Solutions containing 10 μM MPG were incubated in buffer containing DNA at concentrations ranging from 0 to 19.2 μM , which should have been more than enough to fully quench the MPG fluorescence, according to the previous work.

Surprisingly, we could not reproduce the previous results. The MPG fluorescence decreased only slightly with the addition of DNA (fig. 2.4A), even at the highest concentration, and this was quite possibly due to photobleaching of the fluorophore. There was no indication that the DNA and MPG were forming noncovalent complexes.

Because it contains a cysteamide moiety (table 2.1), MPG may form covalently linked homodimers under oxidizing conditions that may interfere with its binding to DNA. The above experiment was repeated for pTAT in solutions with and without

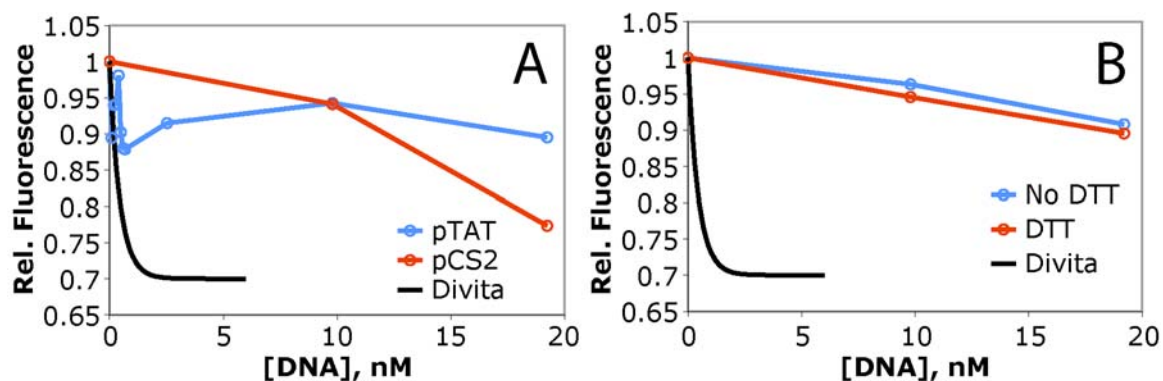


Fig. 2.4. Fluorescence quenching of 10 μM MPG due to complexation with plasmid DNA. The black curves approximate the data reported by Divita and co-workers [47]. *A*, Fluorescence quenching with two different plasmids. *B*, Fluorescence quenching by pTAT with and without 30 μM DTT.

30 μM dithiothreitol (DTT) to prevent the formation of disulfide bonds. However, the presence of DTT had no influence on the fluorescence quenching (fig. 2.4B).

It is unclear why our results differed so significantly from those seen previously. Despite this, we proceeded with experiments attempting to use noncovalent complexes with MPG to deliver both plasmid DNA and tRNA to living cells.

Optimization of Cell Culture Conditions

Because of the cost of generating peptide by solid-phase synthesis, it is important to develop an experimental system that minimizes the amount of the peptide required for application to cultured mammalian cells. Even in the smallest commonly used culture dishes, which are 35 mm in diameter, the amount of medium necessary to maintain healthy cells is ~ 3 mL. Given that MPG experiments required concentrations of ~ 100 μM , if we were to use these dishes, the amount of MPG needed would be on the order of 1 mg per dish, which is excessive. Therefore, we sought a culture system that

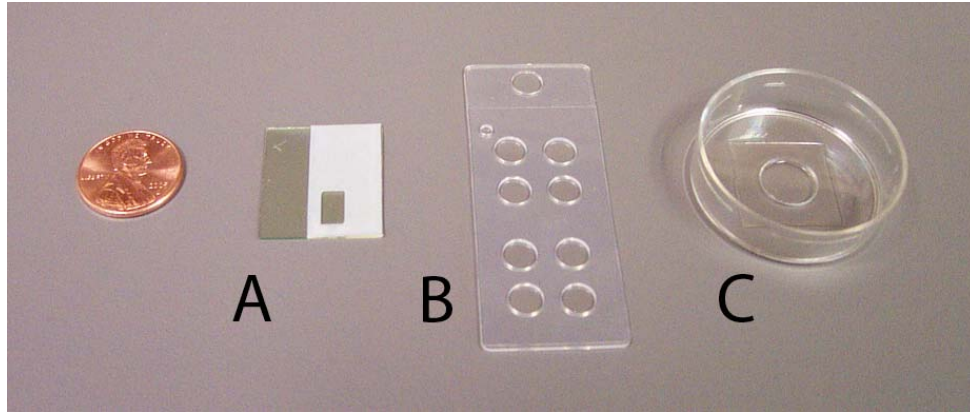


Fig. 2.5. The three small-well containers used to grow cells. *A*, Epizap slide, consisting of a glass cover slip coated with an indium-tin oxide alloy and a Teflon cover that surrounds a 4 x 7 mm rectangular well. *B*, CultureWell slide, consisting of a glass slide covered with a silicone gasket that surrounds eight wells, each with a diameter of 5 mm. *C*, MatTek glass-bottom dish, consisting of a 35 mm culture dish with a 10 mm hole. A glass cover slip is mounted at the bottom of the hole. The penny is shown for scale.

allowed for the growth of cells in tiny wells, on the order of 30 μL instead of 3 mL, requiring only 10 μg of MPG per well.

Possibilities for an appropriate culture system included Epizap slides, CultureWell slides, and MatTek glass-bottom dishes (fig. 2.5), all of which contain wells that can be fully covered with 50 μL or less of medium. To determine the ideal system, CHO-K1 cells were cultured in each type of container, and after 24–48 hours of growth, visualized to determine which had the healthiest appearance.

The best system was found to be the MatTek dishes. The cells on the glass cover slip inside the well grew nicely and remained healthy (fig. 2.6A).

The cells on the Epizap slides also remained generally healthy (fig. 2.6B), although often their health was noticeably compromised compared to those in the MatTek dishes, as noted previously [42]. These slides were designed specifically for use with the Epizap electroporation system, which transfects cells with DNA from the bath solution

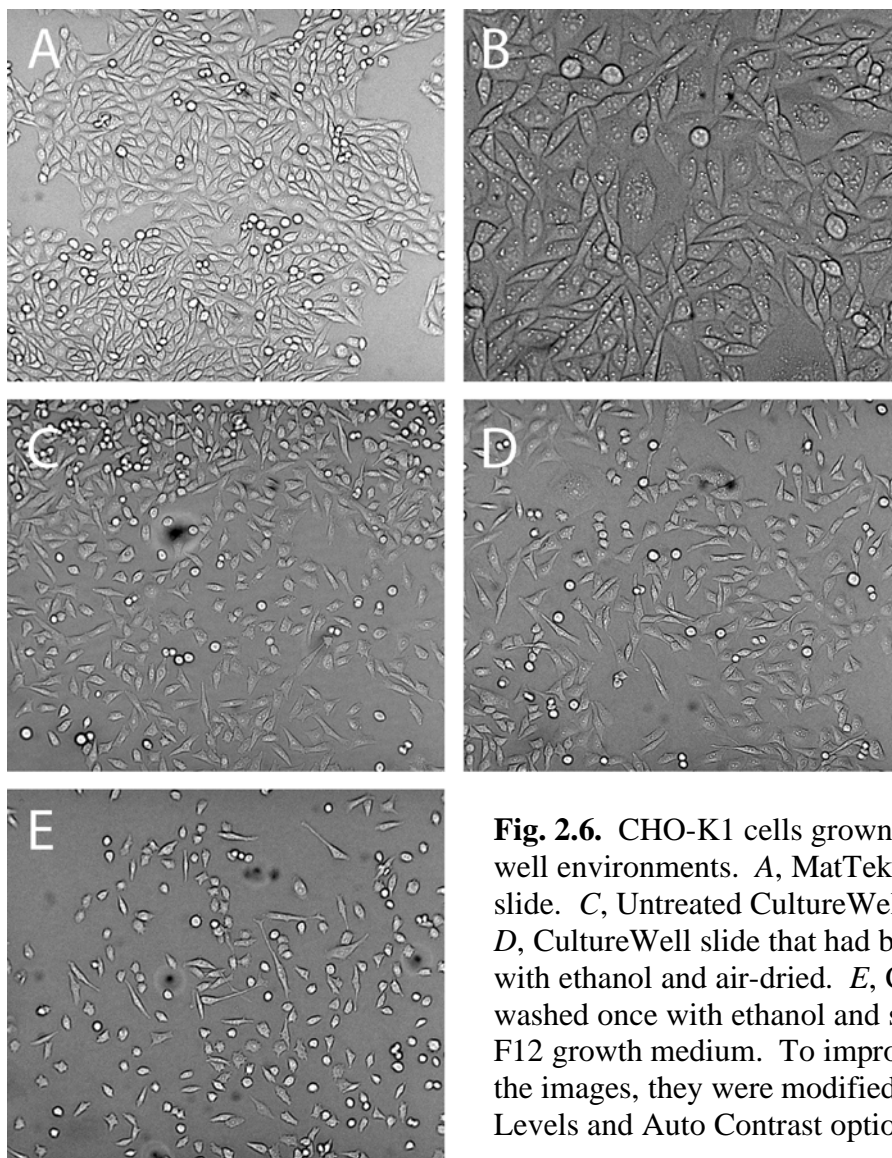


Fig. 2.6. CHO-K1 cells grown in different small-well environments. *A*, MatTek dish. *B*, Epizap slide. *C*, Untreated CultureWell slide. *D*, CultureWell slide that had been washed once with ethanol and air-dried. *E*, CultureWell slide washed once with ethanol and several times with F12 growth medium. To improve the quality of the images, they were modified with the Auto Levels and Auto Contrast options in Photoshop.

by the application of electrical pulses, and as such, were required in all the experiments in which the cells were subjected to the Epizap protocol. The probable cause of the slight decrease in health was the coating of indium-tin oxide on the slides, used because the slide itself is one of the electrodes for electroporation.

The CultureWell slides provided the harshest environment. Many cells in the wells died, and even those that looked healthy did not appear to be dividing, as they were all spaced relatively far apart (fig. 2.6C–E). Often, this was true even when cells that

were in the bottom of the dish outside of the wells looked reasonably healthy, indicating that the environment inside the wells was itself detrimental to the cells. The slides were also subjected to different sterilization treatments before the addition of cells in order to determine if this would improve cell health. Some slides were rinsed in ethanol and allowed to air dry in the laminar flow hood overnight, and some were rinsed once in ethanol and several times in growth medium. None of these treatments had any effect on cellular health. The poor health was unexpected, because these slides were specifically developed to culture mammalian cells in small volume compartments.

Therefore, in most experiments that did not require electroporation, MatTek dishes were used. When electroporation was required and in a few other early experiments, the Epizap slides were used.

Because the purpose of the small-well containers was to minimize the amount of solution the cells needed to survive, it was important to make sure that the wells of the MatTek dishes provided a healthy environment for the cells even when covered with a small amount of medium. Therefore, cells growing in a MatTek dish were subjected to conditions they were likely to encounter during experiments with MPG, and their health was monitored. CHO-K1 cells were cultured in a MatTek dish for 2 days in a normal amount of F12 growth medium (2 mL). The growth medium was removed from the dish, and only 30 μ L of serum-free F12 was applied to the well. The cells were incubated for an hour before 2 mL of fresh F12 growth medium was added to the dish. From visual inspection, it was clear that the health of the cells in the well was not compromised by this procedure. They remained healthy throughout the low-volume incubation and were still healthy 24 hours later.

Finally, it was important to optimize the seeding conditions for the cell cultures. Using too many seed cells would cause the culture to become overgrown and unhealthy, while using too few would reduce transfection efficiency. Therefore, different numbers of CHO-K1 and HEK293 cells were used to seed cultures in MatTek dishes, and the culture densities were observed after 72–96 hours of growth. The optimal seeding numbers were found to be 2×10^5 and 1×10^5 cells for CHO-K1 and HEK293 cells, respectively. Therefore, these numbers of cells were used to seed cultures for subsequent experiments.

Experiments with peptides began once the cell culture conditions were optimized.

DNA Delivery by MPG

Previous work has demonstrated that the application of MPG/DNA complexes is an effective technique for transfection of many types of mammalian cells [46–49]. The transfection procedure consisted simply of the preincubation of MPG with plasmid in a charge ratio of 5/1 (positive charges to negative charges) and addition to cells in culture, which resulted in robust expression of the gene on the plasmid [47].

Our experiments utilized a wild-type EGFP reporter gene inserted into the pCS2 plasmid (wt-EGFP DNA). Solutions of 100 μ M MPG with 6.25, 12.5, 25, or 50 nM DNA (charge ratios of 2.2/1, 4.4/1, 8.9/1, and 17.8/1) were prepared in serum-free F12. The solutions were incubated for 10 minutes and applied to CHO-K1 cells for 60 minutes before dilution in F12 growth medium. The cells were imaged by fluorescence microscopy 24–48 hours later.

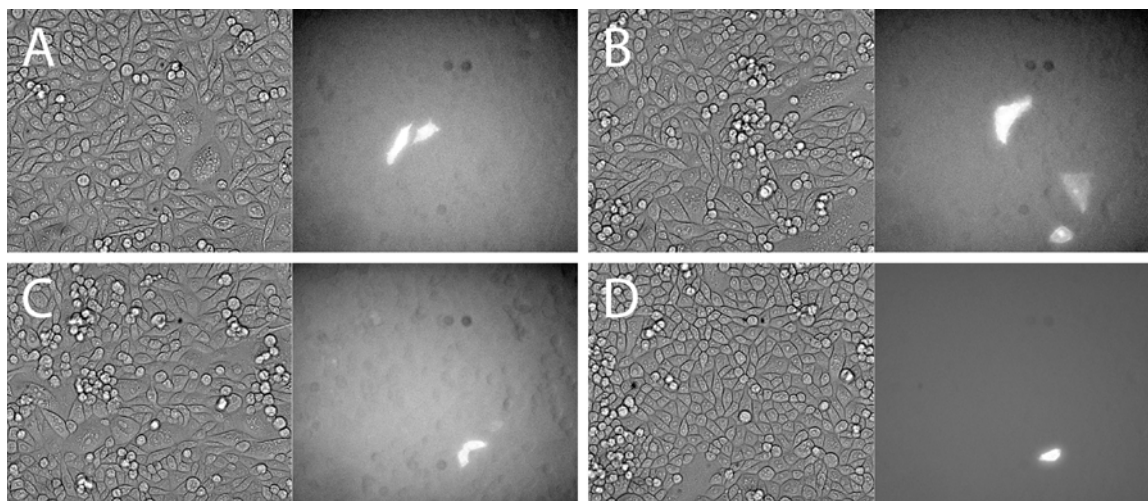


Fig. 2.7. CHO-K1 cells treated with solutions containing MPG and wt-EGFP DNA. The MPG/DNA ratios were 100 μ M/25 nM (4.4/1 charge ratio) (A–B) and 100 μ M/12.5 nM (8.9/1 charge ratio) (C–D). Corresponding bright field and fluorescent images are paired. Exposure times for the fluorescent images were 1 s (A–B), 4 s (C), or 0.5 s (D). To improve the quality of the images, they were modified with the Auto Levels and Auto Contrast options in Photoshop.

The cells remained healthy throughout the experiment, indicating that 100 μ M MPG is not toxic, in agreement with previous work. Although a few cells expressed EGFP, the vast majority did not (fig. 2.7). Thorough inspection of all the cultures revealed that of the thousands of cells, just 11 were fluorescent. Eight were from the 4.4/1 sample (fig. 2.7A–B), three were from the 8.9/1 sample (fig. 2.7C–D), and no fluorescent cells were found in either the 2.2/1 or 17.8/1 sample. However, given the extremely low efficiency of transfection, the numbers of fluorescent cells cannot be meaningfully compared. Subsequent attempts of this experiment confirmed these results, which suggests that contrary to previous reports, transfection by MPG is not efficient at all. In fact, it is quite possible that a mechanism completely independent of MPG resulted in the very limited uptake of plasmid DNA into the cells.

Other DNA Delivery Techniques

Although MPG failed as a delivery vector for plasmid DNA, it was still possible that it could be used to deliver tRNA. Compared to plasmid DNA, tRNA is much smaller and has a very different three-dimensional structure. However, testing this hypothesis required a suitable method to deliver DNA. Many methods exist for transfecting cultured cells, including electroporation and transfection reagents, both of which were tried. Specifically, the Epizap electroporation system was used because it is compatible with the small volume wells necessary for the peptide experiments, and PolyFect Transfection Reagent (PF) was used because it was specifically designed for transfection of common cell lines such as CHO and HEK293.

Transfection of CHO-K1 cells with wt-EGFP DNA was performed with both Epizap and PF, and transfection of HEK293 cells was also performed with PF. Fluorescence microscopy was used to determine the percentage of fluorescent cells, indicating how effectively each technique delivered DNA. In general, Epizap led to high transfection efficiencies (~50%; fig. 2.8A) but often resulted in high cell death. Previous work in our lab has shown that attempts to optimize the electroporation conditions did not significantly improve the health of the cells [42].

In contrast, PF generally led to healthier cells but lower transfection efficiencies (~12% in CHO-K1, ~40% in HEK293; fig. 2.8B–C). We performed experiments to optimize the amount of PF and the amount of DNA in CHO-K1 cells. First, transfection was performed with different amounts of PF and DNA such that the ratio of the two reagents remained nearly the same: 3 μ L PF/0.5 μ g DNA, 10/1.5, 30/5, and 60/10 (fig. 2.9). Exposure to 30 or 60 μ L PF killed all of the cells, and the transfection

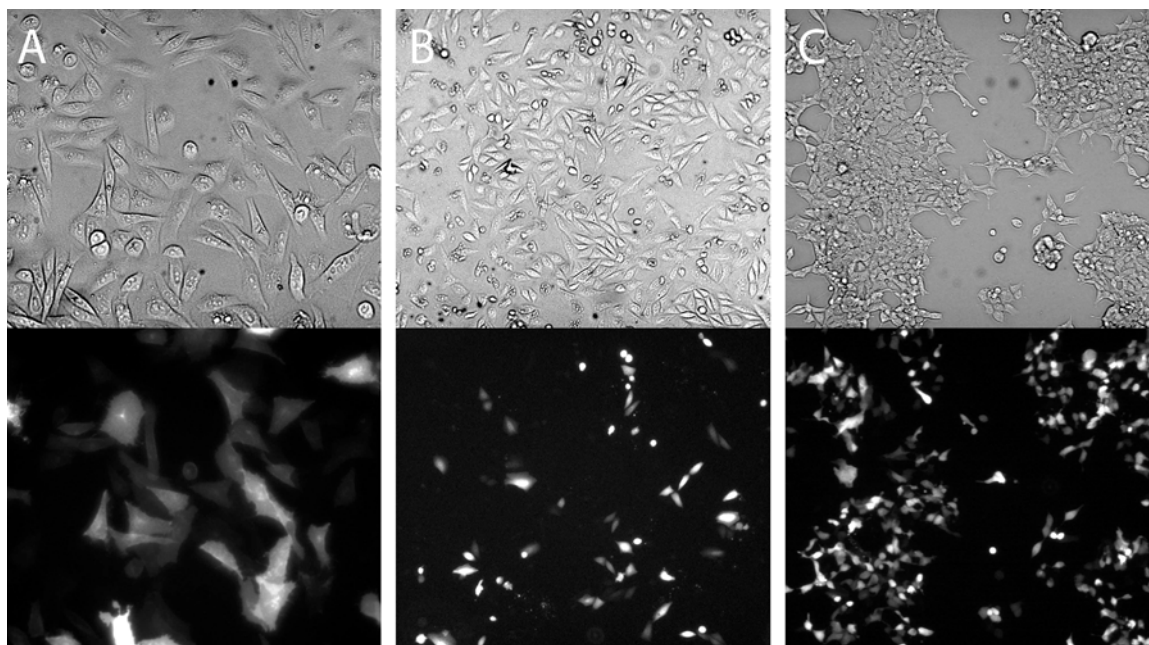


Fig. 2.8. Transfection efficiency for Epizap in CHO-K1 (A) and PolyFect in CHO-K1 (B) and HEK293 cells (C). Corresponding bright field and fluorescent images are paired. Exposure times for fluorescent images were 1 s (A), 0.5 s (B), or 0.3 s (C). To improve the quality of the images, they were modified with the Auto Levels and Auto Contrast options in Photoshop.

efficiency with 3 μL PF was lower than that with 10 μL PF. Second, transfection was performed with 10 μL PF and 0.75, 1.5, 3.0, or 5.0 μg DNA (fig. 2.10). The efficiency was highest for the cells that received 1.5 and 3.0 μg DNA (fig. 2.10B–C). These results confirmed that the manufacturer recommendations (10 μL PF and 1.5 μg DNA) were the best for transfection in our system, and therefore these amounts were used in further experiments that utilized PF for transfection.

Because neither of these methods was significantly better than the other in both preservation of cell health and transfection efficiency, both of them were used to deliver DNA in MPG/tRNA delivery experiments.

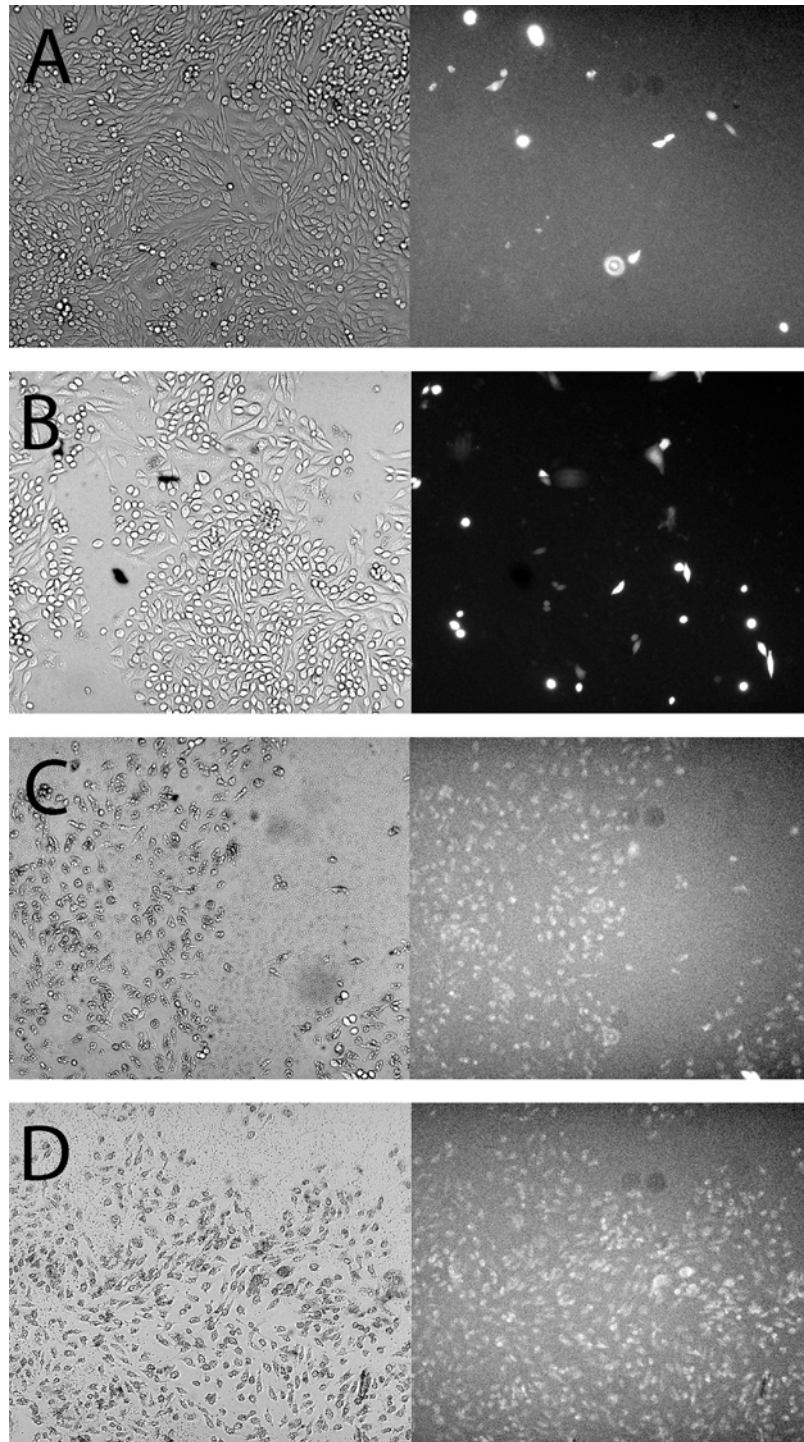


Fig. 2.9. Expression of EGFP in CHO-K1 cells transfected using different amounts of PF and wt-EGFP DNA. PF/DNA ratios (in $\mu\text{L}/\mu\text{g}$) were 3/0.5 (A), 10/1.5 (B), 30/5.0 (C), and 60/10.0 (D). The cells in C and D are all dead. Corresponding bright field and fluorescent images are paired. Exposure times for all fluorescent images were 2 s. To improve the quality of the images, they were modified with the Auto Levels and Auto Contrast options in Photoshop.

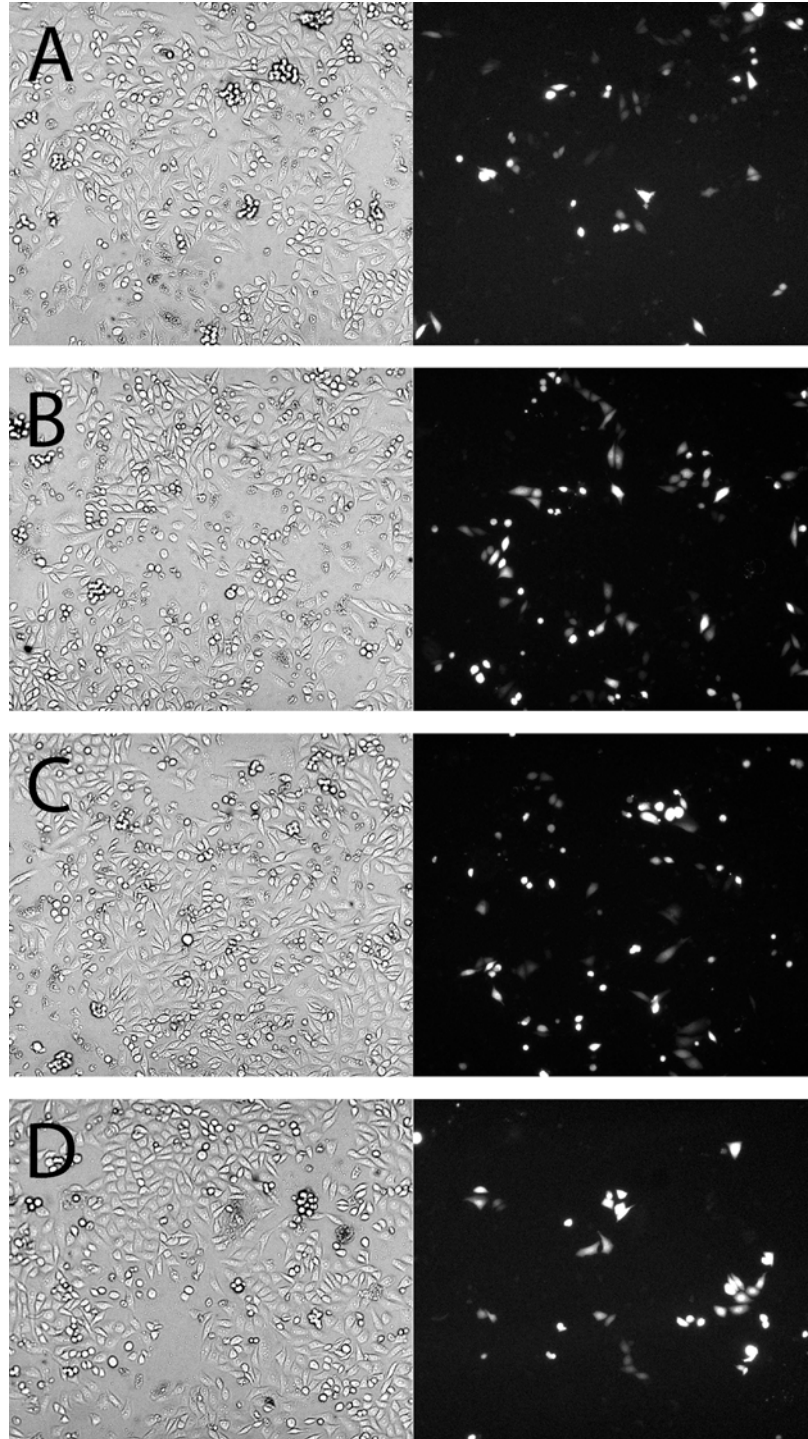


Fig. 2.10. Expression of EGFP in CHO-K1 cells transfected using 10 μ L PF and 0.75 (A), 1.5 (B), 3.0 (C), or 5.0 μ g wt-EGFP DNA (D). Corresponding bright field and fluorescent images are paired. Exposure times for all fluorescent images were 0.5 s. To improve the quality of the images, they were modified with the Auto Levels and Auto Contrast options in Photoshop.

MPG Delivery of tRNA

The assay to detect tRNA delivery into mammalian cells, previously developed in our lab, is outlined in fig. 2.11 [13]. It requires two components: an S29TAG-mutant EGFP gene, in which the amber stop codon (TAG) has replaced a serine codon, and the human serine amber suppressor (HSAS) tRNA [50]. HSAS is an unusual tRNA in that the anticodon was mutated to recognize the amber stop codon instead of its natural serine codon, but because seryl-tRNA synthetases do not use the anticodon as a recognition element, it can still be charged with serine like the natural tRNA^{Ser} molecules. Under normal circumstances, the translation of the S29TAG-EGFP gene would terminate at position 29 due to the TAG codon, and no fluorescent protein would be produced. However, HSAS can rescue expression of this gene because it is charged with serine but recognizes the TAG codon, thereby delivering the wild-type amino acid at position 29, resulting in a wild-type EGFP protein. Therefore, the presence of HSAS can be easily detected in cells expressing S29TAG-EGFP by fluorescence microscopy. Cells that contain HSAS are fluorescent, but those lacking HSAS are not.

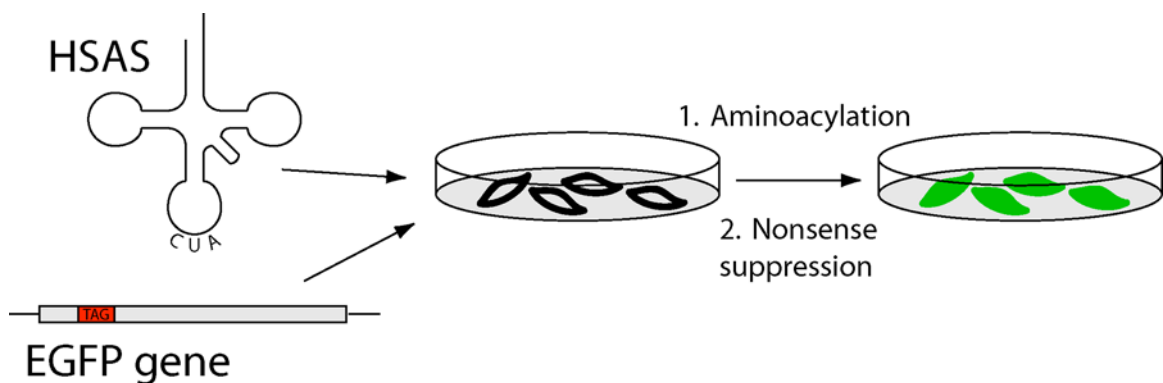


Fig. 2.11. The HSAS assay for tRNA delivery. Cells that contain a gene for a mutant EGFP with an internal TAG stop codon will not produce EGFP because the translation will terminate. However, if HSAS is delivered to the cells, aminoacylation by the endogenous synthetases and nonsense suppression at the TAG site will yield wild-type EGFP, detectable by fluorescence.

To determine if MPG could be used to deliver tRNA, cells were transfected with S29TAG-EGFP DNA using Epizap or PF, and MPG/HSAS complexes were applied ~24 hours later. 24–48 hours after HSAS application, the cells were observed for EGFP fluorescence. In contrast to the MPG/DNA complexation experiments, the initial results were somewhat promising. Transfection by Epizap was attempted first because it was able to deliver more DNA. CHO-K1 cells were transfected with S29TAG-EGFP, and precomplexed 51 μ M MPG/0.5 μ M HSAS (5/1 charge ratio) solution was applied to the cells. The application of the MPG and HSAS resulted in many fluorescent cells (fig. 2.12A–B), whereas the control samples missing one or both components had essentially no fluorescence (fig. 2.12C–E). This suggested that MPG effectively delivered HSAS into the cells.

Unfortunately, this result could not be reliably reproduced, because of the inconsistency of the cell health and transfection efficiency after Epizap treatment. No other attempts using Epizap transfection produced more than one or two healthy fluorescent cells.

Transfection with PF was then used because of the improvement in cell health with this technique. These experiments had the additional complication that the cells transfected with S29TAG-EGFP by PF remained healthy and produced small amounts of EGFP without HSAS. This occurred by a process known as readthrough, in which the translational machinery occasionally skipped over the TAG codon or erroneously inserted another amino acid instead of terminating the translation. When MPG/HSAS complexes were applied to the cells, there was obvious fluorescence (fig. 2.13A–B), but it was never significantly higher than that from readthrough (fig. 2.13C–E), even though several

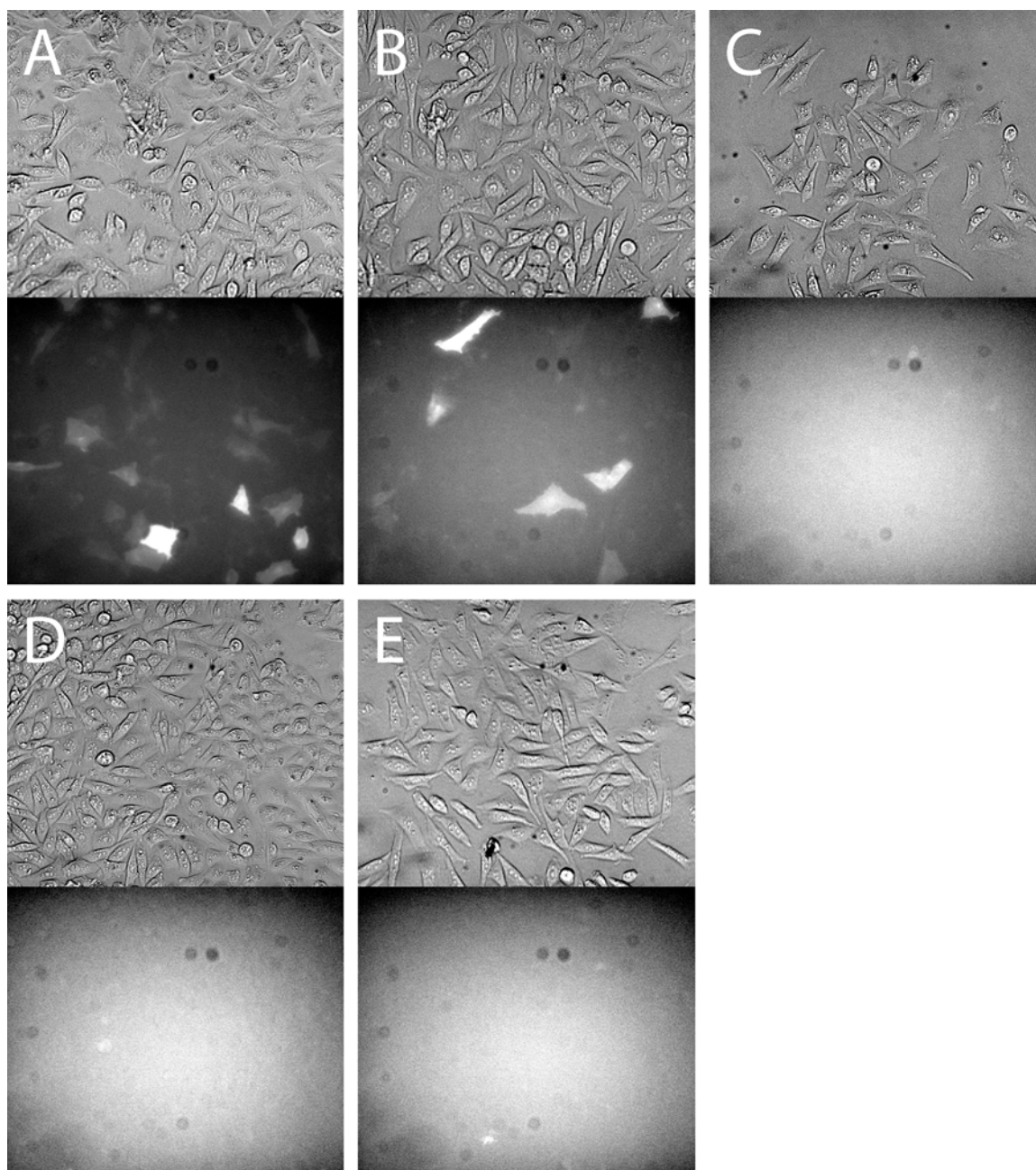


Fig. 2.12. *A–B*, Expression of EGFP in CHO-K1 cells transfected with S29TAG-EGFP DNA and incubated with solutions of 51 μM MPG/0.5 μM HSAS (5/1 charge ratio).
C–E, Control cultures that were incubated with 51 μM MPG only (*C*), 0.5 μM HSAS only (*D*), and F12 medium only (*E*). These results suggested that we had successfully delivered tRNA with MPG, but they could not be reproduced (see fig. 2.13).
Corresponding bright field and fluorescent images are paired. Exposure times for all fluorescent images were 5 s. To improve the quality of the images, they were modified with the Auto Levels and Auto Contrast options in Photoshop.

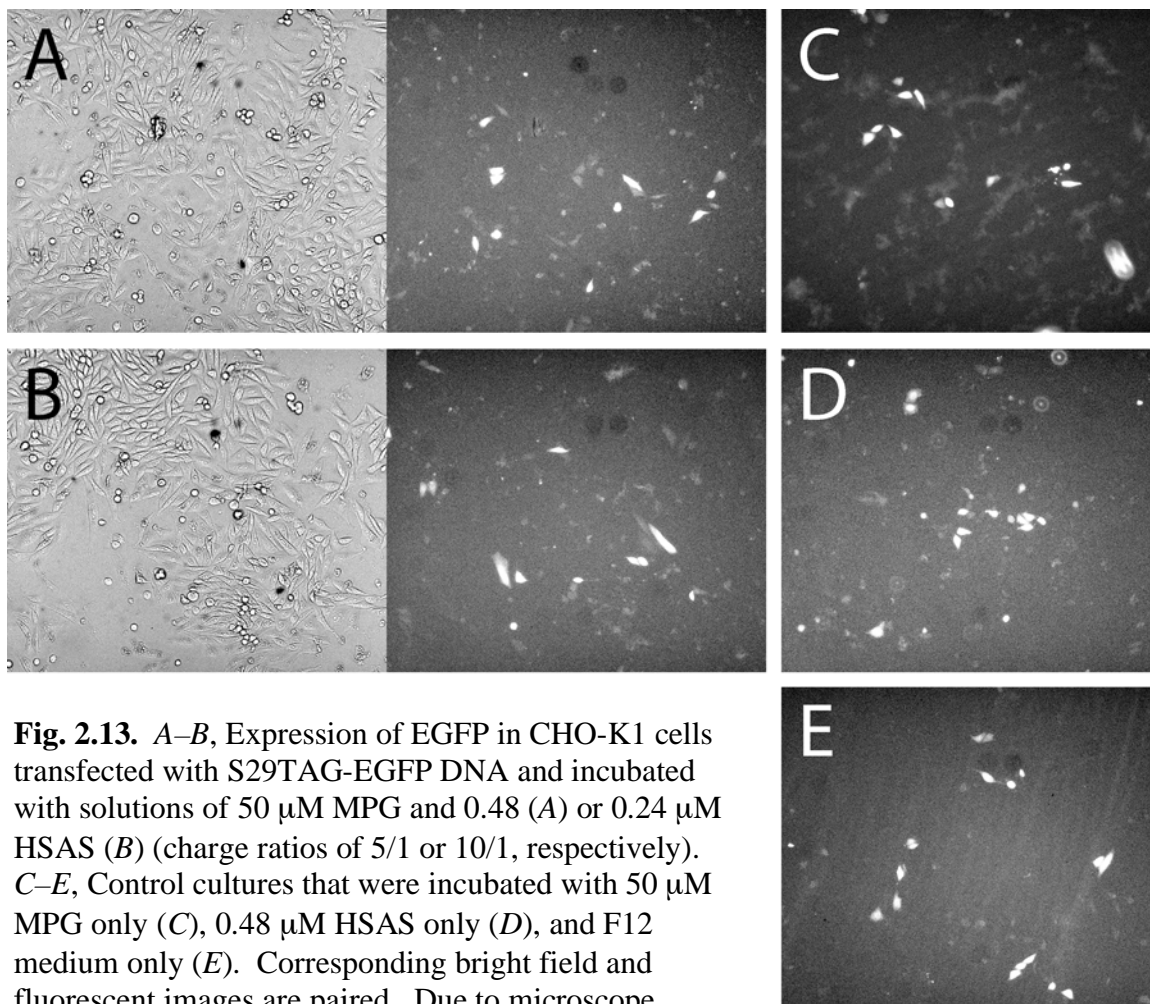


Fig. 2.13. *A–B*, Expression of EGFP in CHO-K1 cells transfected with S29TAG-EGFP DNA and incubated with solutions of 50 μM MPG and 0.48 (A) or 0.24 μM HSAS (B) (charge ratios of 5/1 or 10/1, respectively). *C–E*, Control cultures that were incubated with 50 μM MPG only (C), 0.48 μM HSAS only (D), and F12 medium only (E). Corresponding bright field and fluorescent images are paired. Due to microscope malfunction the bright field images for the fluorescent images in *C–E* were not obtained. Exposure times for all fluorescent images were 2 s. To improve the quality of the images, they were modified with the Auto Levels and Auto Contrast options in Photoshop.

attempts were made to optimize the charge ratio and amount of HSAS in the delivery complexes. Therefore, it could not be definitively stated that the MPG delivered HSAS to the cells. This result was observed in both CHO-K1 and HEK293 cells.

In summary, we were unable to reproduce any of the results of Divita and co-workers [46–48]. We failed to observe MPG and DNA complexation by fluorescence, and we could not use MPG to deliver plasmid DNA or RNA into cells. It is very

puzzling that our results differed so drastically from theirs. A possible explanation is that MPG is a cell-type specific carrier, unable to deliver to CHO or HEK cells. None of the previous reports of Divita and co-workers involved these cell types. Also, it is interesting that so far, no other research group has reported using MPG to deliver nucleic acids into cells, indicating that MPG may be functional as a delivery agent only under very specific conditions. In any case, we concluded that the method of using MPG to form noncovalent complexes with tRNA for delivery into cells is not a viable strategy in our experiments.

Antp Delivery of tRNA

One other noncovalent complexation experiment was performed. Antp was used instead of MPG as the peptide carrier to delivery tRNA into cells. PF was used to transfect CHO-K1 and HEK cells with S29TAG-EGFP DNA, and solutions containing 50 μ M Antp and 0.80 μ M HSAS (5/1 charge ratio) were applied to the cells. As seen with the MPG experiments above, the cells of the Antp/HSAS sample (fig. 2.14A,C) had no more fluorescence than those of control cells that received no peptide or tRNA (fig. 2.14B,D). Antp, like MPG, failed as a delivery agent, and the fluorescence seen in the samples was due simply to readthrough.

Therefore, we concluded our experiments involving noncovalent complexation with peptides, never having definitively observed tRNA delivery to the mammalian cells. It was decided that this approach is not a viable option to deliver tRNA.

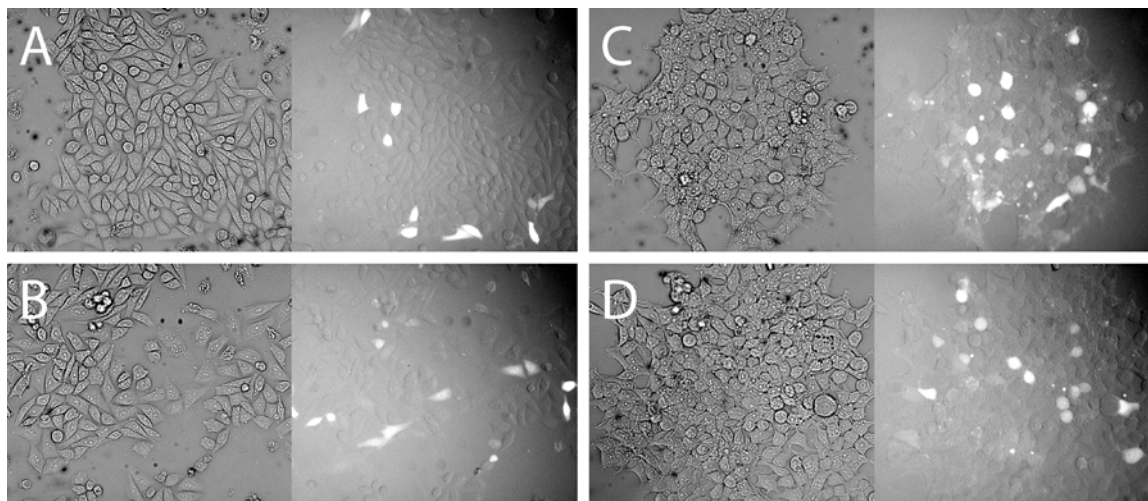


Fig. 2.14. *A–B*, Expression of EGFP in CHO-K1 cells transfected with S29TAG-EGFP DNA and incubated with solutions of 50 μ M Antp and 0.80 μ M HSAS (5/1 charge ratio) (*A*) or F12 only (*B*). *C–D*, Expression of EGFP in HEK293 cells transfected with S29TAG-EGFP DNA and incubated with solutions of 50 μ M Antp and 0.80 μ M HSAS (5/1 charge ratio) (*C*) or F12 only (*D*). Corresponding bright field and fluorescent images are paired. Exposure times for all fluorescent images were 2 s. To improve the quality of the images, they were modified with the Auto Levels and Auto Contrast options in Photoshop.

Preparation of Tat-eEF1A Fusion Protein

The final approach to utilize PTDs to deliver tRNA to cells is the production of a chimera of a PTD and a tRNA-binding protein, specifically the Tat PTD and the eukaryotic elongation factor eEF1A (formerly known as EF-1 α). Fusing proteins and PTDs has been shown to impart them with the PTD translocation properties [24–26], even allowing them to also transport sufficiently tight binding partners of the protein [51]. In this manner, the Tat-eEF1A fusion protein can be mixed with tRNA outside the cell, and the entire complex can be internalized by translocation of the Tat (fig. 2.15).

Furthermore, the ternary complex of eEF1A, GTP, and aminoacyl-tRNA is recruited by the ribosome for tRNA delivery to the ribosomal A site [52, 53]. The formation of this complex is a necessary step for translation, so prebinding the unnatural aminoacyl-tRNA to GTP-activated eEF1A and delivering the complex into the cells

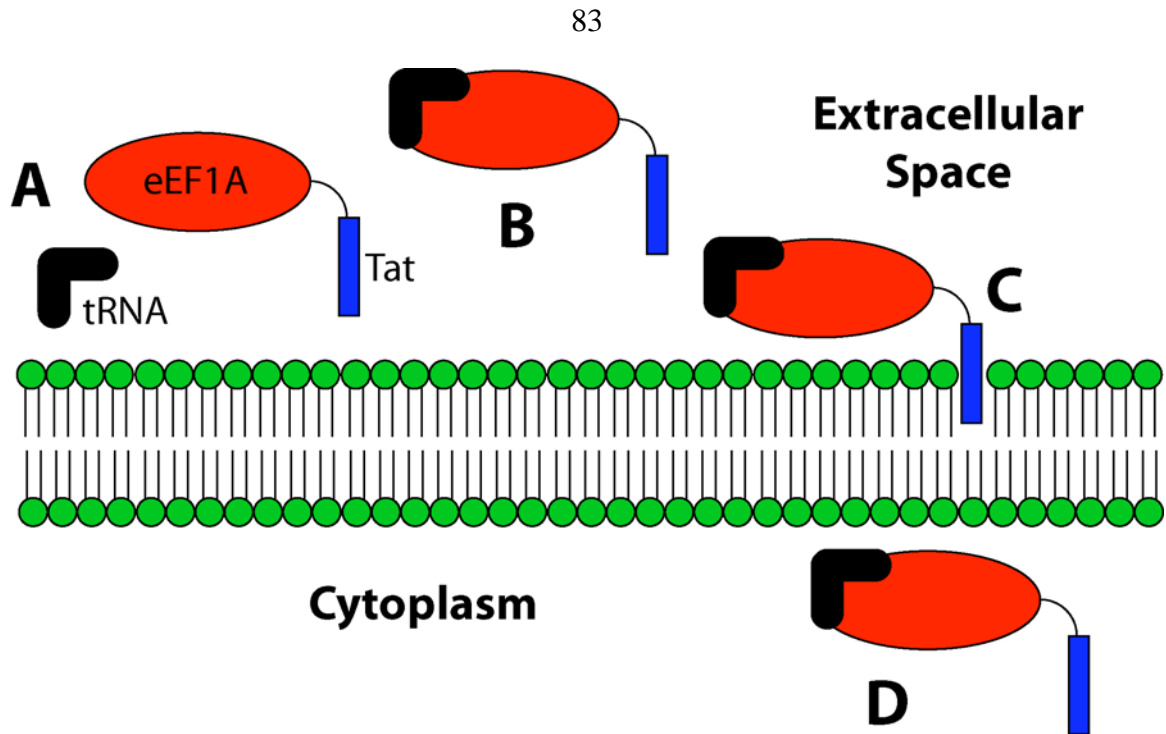


Fig. 2.15. Delivery of tRNA using Tat-eEF1A. The tRNA and Tat-eEF1A are mixed in the external solution (A) and bind together (B). Translocation of the Tat peptide (C) internalizes the entire complex (D).

could make nonsense suppression more efficient. The tRNA molecules would be delivered directly to the ribosome, eliminating the need to encounter an endogenous eEF1A inside the cell.

The binding affinities for the eEF1A and natural aminoacyl-tRNAs range from ~1 to 10 nM, which probably is sufficiently high to maintain a stable complex during translocation into the cell [54]. However, studies on the prokaryotic homologue EF1A (formerly known as EF-Tu), which has RNA binding properties similar to eEF1A [54], have demonstrated that the aminoacyl moiety of the charged tRNA strongly influences its binding affinity. The affinities of misacylated tRNA molecules cover a much broader range, from less than 100 pM to more than 300 nM [55, 56]. It is difficult to predict how a specific unnatural aminoacyl-tRNA will bind to eEF1A, but hopefully the complex can

survive intact throughout the delivery into the cell, even if the binding affinity is significantly weaker than the normal interactions between eEF1A and aminoacyl-tRNA.

There are several steps involved in producing recombinant Tat-eEF1A. First, the genetic construct must be generated and transformed into bacteria. Second, the protein must be overexpressed and purified from the numerous bacterial proteins. Finally, if the protein is not already in its native conformation, appropriate refolding conditions must be determined.

Generation of the Fusion Protein Construct, Transformation, and Overexpression

To generate the fusion protein construct, the eEF1A gene from *Xenopus laevis* was subcloned into the pTAT plasmid, a vector that was designed to allow for the easy generation of Tat fusion proteins [57]. The fact that this gene is from *Xenopus*, not of mammalian origin, is not a concern even in a mammalian expression system, because eEF1A is one of the most conserved proteins known [53]. For example, the *Xenopus* and human proteins are 96% identical. The plasmid containing the eEF1A insert was transformed into the Rosetta(DE3) bacterial cell line, which is effective for the overexpression of proteins of eukaryotic origin such as eEF1A. The Rosetta(DE3) line is identical to the BL21(DE3) *E. coli* cell line, except its genome is supplemented with six tRNA genes with anticodons common in eukaryotes but rare in prokaryotes.

Tat-eEF1A was overexpressed, and several different harvesting procedures were attempted. The protein formed inclusion bodies that needed to be purified and solubilized, as observed previously for an EF1A/eEF1A chimera [58], so an inclusion

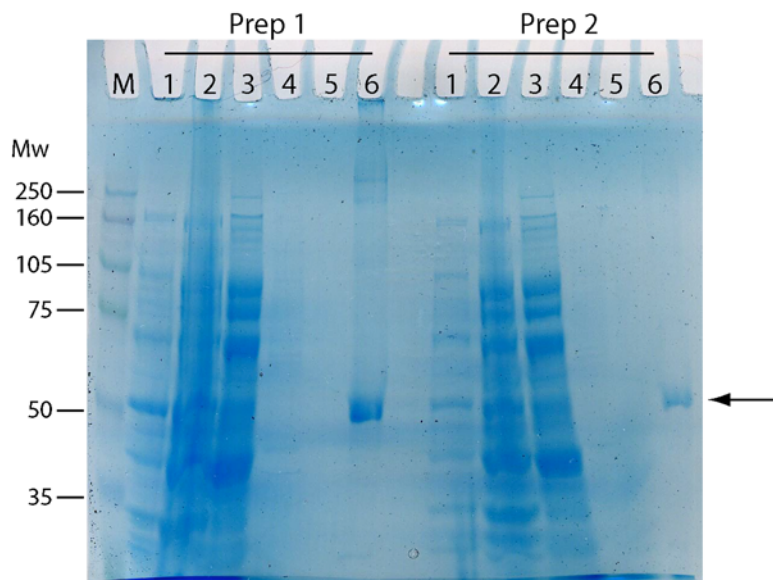


Fig. 2.16. Coomassie-stained polyacrylamide gel showing the protein harvested at different stages of inclusion body purification. Two individual preparations are shown; the same step for each preparation is marked with the same lane number.

Lane M: rainbow markers, with molecular weights at left. Lane 1: uninduced control sample. Lane 2: induced control sample. Lane 3: supernatant 1. Lane 4: supernatant 2.

Lane 5: supernatant 3. Lane 6: inclusion body pellet solubilized in 8 M guanidinium chloride. See methods for the details of the purification. The Tat-eEF1A is marked by the arrow, clearly in a pure, concentrated solution in lane 6.

body preparation procedure was used. This method yielded a large amount of protein, producing 20 to 100 mg per liter of bacterial culture (fig. 2.16).

The presence of Tat-eEF1A in inclusion bodies was fortunate because the relatively simple preparation of the inclusion bodies yielded almost completely pure protein, as inclusion bodies contain only trace amounts of the endogenous bacterial proteins (fig. 2.16). However, it added the complication that the denatured protein needed to be refolded into an active form, and suitable refolding conditions could only be determined by trial and error.

Refolding

The most common method of refolding solubilized, denatured proteins is rapid dilution in buffer containing additives that enhance refolding, such as DTT, arginine (Arg), guanidinium chloride (GuCl), and glycerol. Buffers of eight different compositions were tried: all possible combinations of buffers that contained 0 or 400 mM Arg, 0 or 500 mM GuCl, and 0 or 20% glycerol. 1–2 mg Tat-eEF1A was diluted in 80 mL of each refolding buffer and stirred gently for eight hours. The solution was filtered through a 0.2 μm filter to remove protein that had reaggregated, and was then concentrated.

Upon dilution of the protein, it was immediately obvious that the solutions that contained neither Arg nor GuCl did not promote refolding, because the protein precipitated out and formed a cloudy mixture. However, precipitates were not visible in the other six solutions, so after filtration and concentration, the protein yields were determined by sodium dodecyl sulfate-polyacrylamide gel electrophoresis (SDS-PAGE). The results indicated that three buffers—the Arg/glycerol, Arg/GuCl/glycerol, and Arg/GuCl solutions—all prevented reaggregation of the protein and resulted in good yields of concentrated protein (fig. 2.17). The other three other buffers—the GuCl/glycerol, Arg, and GuCl solutions—did not. Thus, protocols for the purification and solubilization of Tat-eEF1A were determined.

The protein, however, was not stable in solution at high concentrations for very long, even when stored at 4 °C. PAGE performed even one or two days after purification and concentration showed that all the protein had been degraded. It was not clear what mechanism caused the degradation. One possibility is that the inclusion bodies contained

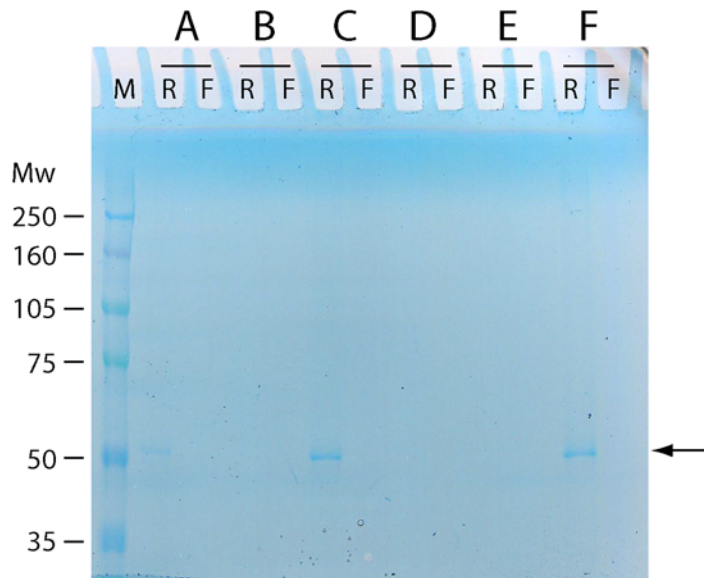


Fig. 2.17. Coomassie-stained polyacrylamide gel of the retentates (R lanes) and filtrates (F lanes) following the concentration of Tat-eEF1A in several refolding buffers. Buffer compositions were 400 mM Arg/20% glycerol (A), 500 mM GuCl/20% glycerol (B), 400 mM Arg/500 mM GuCl/20% glycerol (C), 400 mM Arg (D), 500 mM GuCl (E), and 400 mM Arg/500 mM GuCl (F). Lane M: rainbow markers with molecular weights at left. Tat-eEF1A is marked with the arrow, clearly appearing the retentates of three refolding buffers (A, C, and F).

trace amounts of proteases, which, once refolded, acted to proteolyze the Tat-eEF1A.

Even though it seemed unlikely because the refolding buffers contained protease inhibitors, this hypothesis was tested. Further purification of Tat-eEF1A was performed, taking advantage of its 6His tag, in order to completely isolate it from any proteases. The solubilized inclusion bodies were passed through a column of Ni-NTA beads to isolate the desired protein before refolding. However, the problem of the degradation remained even after the Ni-NTA treatment.

Even though the protein could be purified and concentrated, it still remained to be determined if the Tat-eEF1A had folded into a fully functional form, able to bind tRNA. Efforts were made to develop a gel-shift assay, used previously for RNA-binding proteins [59, 60], which would confirm proper refolding of the protein. The binding of tRNA to

the Tat-eEF1A should change the mass/charge ratio significantly, causing the complex to run at a rate distinct from its individual components in a native PAGE gel.

There were a number of challenges to overcome, most notably getting the protein into a native PAGE gel. Like many proteins that bind nucleic acids, eEF1A has a high pI (~9.3), so it is positively charged at neutral pH. Therefore, the unbound protein should not run into the gel under normal electrophoresis conditions, but should simply drift in the buffer towards the cathode. Forcing a negative charge onto Tat-eEF1A by raising the pH of the buffers was not a good solution because it is almost certain to obliterate binding to tRNA.

One interesting option was setting a native PAGE gel in a horizontal container with the sample wells in the center of the gel instead of at the side nearest the cathode. With this “horizontal PAGE” setup, the protein must enter the gel whether it is positively or negatively charged. Although this was an unorthodox method for PAGE electrophoresis, such a gel was loaded with different amounts of Tat-eEF1A and tRNA and later visualized by silver staining (fig. 2.18A–B), but there were several problems. First, the tRNA bands were very obvious (fig. 2.18A), but a protein band was difficult to find. There may have been a very light band from the protein very near the wells towards the anode (fig. 2.18B), but that was opposite of the expected direction for a positively charged protein. To confuse matters, this possible protein band was not seen in a normally poured native PAGE gel (fig. 2.18C), even though the horizontal PAGE results suggested it should have been, so it remained unidentified. Second, it was difficult to handle and stain the horizontal PAGE gel due to its relatively large size. It is unclear if

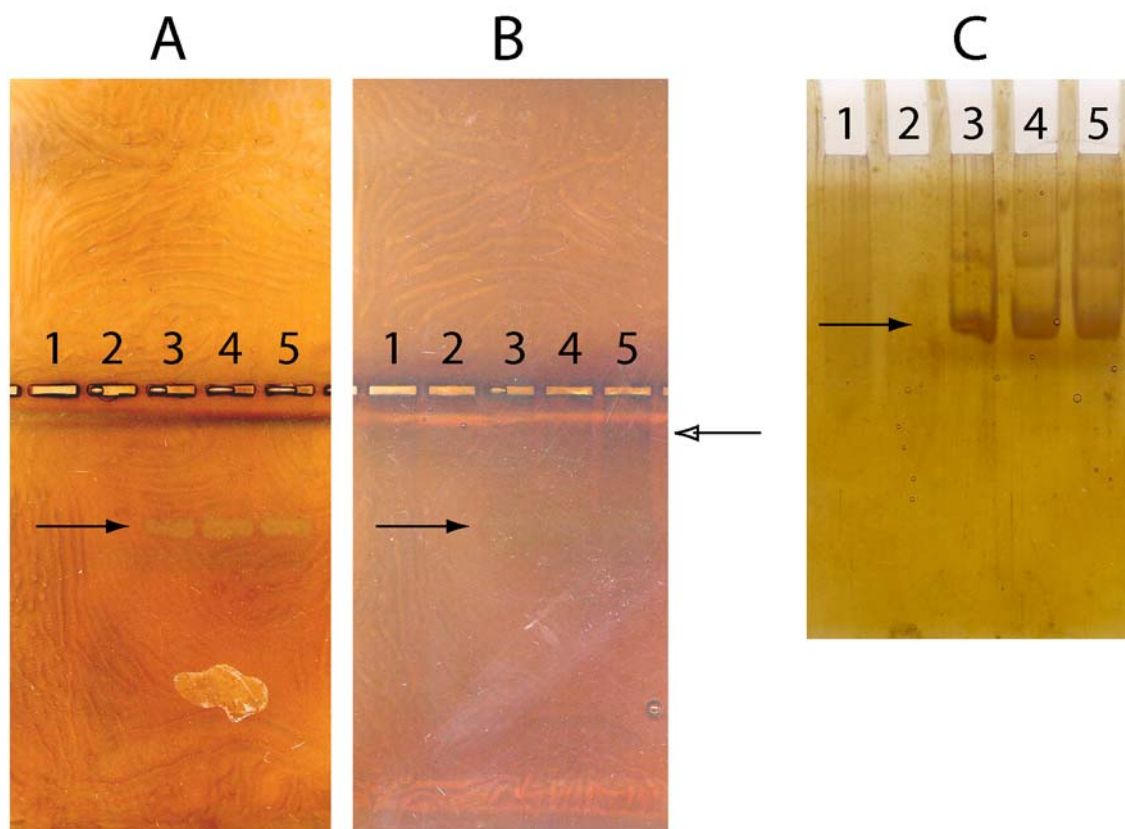


Fig. 2.18. Silver-stained gels from native PAGE of solutions of Tat-eEF1A and HSAS. *A–B*, A gel run horizontally with the wells in the center. *A* and *B* show the same gel at different stages in the development of the silver stain. *C*, A gel run vertically with the wells at the top. All the lanes marked with the same number have identical compositions.

Lane 1: 4 μg Tat-eEF1A. Lane 2: 1 μg Tat-eEF1A. Lane 3: 0.25 μg HSAS.

Lane 4: 1 μg Tat-eEF1A and 0.25 μg HSAS. Lane 5: 4 μg Tat-eEF1A and 0.25 μg HSAS. The black arrow marks the HSAS; the outlined arrow marks a possible protein band, barely discernible in *B* and appearing nowhere else.

the failure to see a protein band was due to degradation, poor staining, or some other factor resulting from the unusual gel technique.

Other methods for detecting the binding of tRNA to Tat-eEF1A were considered but not attempted. Isoelectric focusing, a gel technique that separates proteins based on their pI values, would almost certainly be able to distinguish bound and unbound Tat-eEF1A, but it requires a special apparatus that was not available to us. Also, cross-linking techniques were considered. UV irradiation of a mixture of Tat-eEF1A and

tRNA could result in covalent cross-linking, which would allow for analysis by standard SDS-PAGE. However, cross-linking would probably not be very efficient or quantitative. Even if the protein was properly refolded and bound tRNA, it may not be detectable by this method.

Because of the puzzling problems with degradation of the protein and the lack of a method to determine if the protein was properly refolded, the use of Tat-eEF1A was not a viable strategy for tRNA delivery to mammalian cells.

CONCLUSION

PTDs were expected to be effective vectors for delivering aminoacyl-tRNA to mammalian cells for nonsense suppression. We attempted to develop a PTD-tRNA delivery system by three different approaches: covalent ligation of the two molecules, noncovalent binding, and binding tRNA to a protein linked to a PTD. However, none of these approaches ever successfully transported tRNA into mammalian cells.

To be useful, any PTD technique for tRNA delivery must outperform the relatively easy and effective technique of electroporation. It is possible that such a technique may one day be found. However, this seems much less likely than it did several years ago. The initial reports of the abilities of PTDs to universally cross cell membranes and their seemingly unlimited towing capacity generated much excitement. However, more recent research has shown that the initial results were artifactual and revealed that PTDs were, in fact, relatively limited in their translocation capabilities.

This work was performed concurrently with the optimization of tRNA delivery to mammalian cells by electroporation, which proved to be an effective technique [13].

Because of the success of electroporation, the failure of all three PTD-based approaches, and the diminished likelihood that PTDs could ever be as effective as electroporation, this project was discontinued.

MATERIALS AND METHODS

tRNA Generation

The human serine amber suppressor (HSAS) gene was subcloned into pUC19 as described in [13]. The construct had a T7 transcriptional promoter and a FokI restriction site after 74 bases of the HSAS. The plasmid was amplified and linearized by FokI, and the MegaShortScript Kit from Ambion (Austin, TX) was used for *in vitro* transcription of the 74mer HSAS (the tRNA lacking its two 3' bases).

Thiophosphate Reaction with Maleimide

Alkaline phosphatase (AP) was purchased from Boehringer-Mannheim (Indianapolis, IN), T4 polynucleotide kinase (PNK) from New England Biolabs (Ipswich, MA), and RNase inhibitor from Roche (Indianapolis, IN). ATP-(3-thiophosphate) (ATP- γ -S) was purchased from Boehringer-Mannheim (Indianapolis, IN). N-(1-pyrenyl)maleimide (PM) and 2-mercaptoethanol (2-ME) were purchased from Aldrich. Slide-A-Lyzers were purchased from Pierce (Rockford, IL).

tRNA with a thiophosphate on its 5' end (tRNA-5'-S) was prepared in the following manner. HSAS was prepared by *in vitro* transcription. It was converted to a 5'-OH by AP treatment, with a typical reaction consisting of 100 μ g HSAS, 40 U AP, 80 U RNase inhibitor, and 20 μ L 10x buffer in a total volume of 200 μ L. After

incubating at 50 °C for 2 hours, the protein was removed by PCI treatment, and the tRNA-5'-OH was isolated by ethanol precipitation. This was converted to tRNA-5'-S by PNK treatment, with a typical reaction consisting of 80 µg tRNA-5'-OH, 80 U PNK, 80 U RNase inhibitor, 100 µM spermidine, 500 µM ATP-γ-S, and 20 µL 10x buffer in a total volume of 200 µL. After incubation at 37 °C for 2 hours, the protein was removed by PCI treatment, the free ATP-γ-S was removed by dialysis in Slide-A-Lyzers against 2 L Millipore water (exchanged at 2 hours and 4 hours) for 8 hours, and the tRNA-5'-S was isolated by ethanol precipitation.

A stock solution of 800 µM PM was prepared in 8% DMSO. The DMSO was required to enhance PM's aqueous solubility. Solutions containing various concentrations of 2-ME, ATP-γ-S, and tRNA-5'-S with PM were prepared, in duplicate, in 100 mM phosphate buffer at pH 9.5. Fluorescence emission spectra with an excitation wavelength of 338 nm and a high PMT setting were taken after incubation at room temperature for ~24 hours. The spectra were collected with a SpectraMax Gemini XS fluorescence plate reader using SOFTmax PRO 3.1.2 software.

Noncovalent Complexation Experiments

Materials

Peptides were synthesized on an ABI 433A Peptide Synthesizer and stored as a lyophilized powder. MPG contains a cysteamide at its C-terminus, so it was prepared using a cysteamine 4-methoxytrityl resin, purchased from Calbiochem-Novabiochem (La Jolla, CA). The pTAT plasmid was obtained from Steven Dowdy (Washington University), and the pCS2 plasmid containing the wt-EGFP gene (wt-EGFP DNA) from

Jack Horne (Caltech). The S29TAG-EGFP DNA was obtained by mutation of the wt-EGFP DNA as described previously [13]. Ham's F12 medium and DMEM were purchased from Irvine Scientific (Santa Ana, CA), and CO₂ independent medium was purchased from GIBCO Invitrogen Corporation (Carlsbad, CA). Epizap slides and the Epizap electroporation apparatus were purchased from ASK Science Products (Kingston, Ontario). CultureWell slides were obtained from Grace Bio Labs (Bend, OR). MatTek glass-bottom dishes were obtained from MatTek Corporation (Ashland, MA). PolyFect Transfection Reagent (PF) and the MaxiPrep kits used to isolate plasmids were purchased from Qiagen (Valencia, CA).

Monitoring Complexation with DNA by Fluorescence

Phosphate buffer was prepared with 150 mM NaCl, 18 mM KH₂PO₄, and 5 mM Na₂HPO₄, pH 7.4, the same composition as in [47]. Solutions with 10 μM MPG and 0 to 19.2 μM plasmid DNA (pTAT or wt-EGFP DNA) with or without 30 μM DTT were prepared in phosphate buffer. The fluorescence of the tryptophan residue in MPG was measured at excitation and emission wavelengths of 290 and 345 nm, respectively, at medium PMT, with a SpectraMax Gemini XS fluorescence plate reader using SOFTmax PRO 3.1.2 software.

Cell Culture

CHO-K1 cells were grown in Ham's F12 medium supplemented with fetal bovine serum (10%), glutamine, penicillin, and streptomycin. HEK293 cells were grown in

DMEM with the same additives. The medium with the additives is referred to as “growth medium.” Cells were incubated at 37 °C under 5% CO₂.

CHO-K1 cells were seeded in 8-well CultureWell slides, Epizap slides, or 35 mm MatTek glass-bottom culture dishes. Before seeding, the CultureWell slides were either left untreated, rinsed with ethanol and left to air dry, or rinsed once in ethanol and several times in F12 growth medium. The Epizap slides and MatTek dishes were used without treatment.

During seeding, cells were counted with a bright line counting chamber from Hausser Scientific (Horsham, PA). Usually, 2×10^5 CHO-K1 cells or 1×10^5 HEK293 cells were added to dishes. DNA transfection was usually performed ~48 hours after plating.

DNA Transfection by MPG

CHO-K1 cells were plated on Epizap slides held in 35 mm dishes. The DNA to be transfected was precipitated in ethanol and ammonium acetate and left at –20 °C for at least 1 hour. This was subjected to microcentrifugation at 15,000 rpm and 4 °C for 15 minutes, vacuum dried for 5 minutes, and resuspended in 20 µL serum-free F12 medium with 100 µM MPG. The amounts of DNA used were 6.25, 12.5, 25, or 50 nM wt-EGFP DNA, corresponding to charge ratios of 17.8/1, 8.9/1, 4.4/1, and 2.2/1, respectively. The solution was left for ~30 minutes to allow complexation of the MPG and DNA. 20 µL control solutions of 100 µM MPG only, 25 nM DNA only, and F12 only were also prepared. All medium was removed from the dishes that contained the Epizap slides, and the MPG/DNA solutions were applied to the cells for ~60 minutes at

37 °C. 3 mL F12 growth medium was then added to the dishes, and they were returned to the incubator. The cells were imaged by fluorescence microscopy ~24 hours later.

Transfection by Epizap

CHO-K1 cells were plated on Epizap slides. DNA was precipitated and dried as above and resuspended in CO₂-independent medium to give a final concentration of ~1 µg/µL. The medium was removed from the dishes, and 17 µL of the DNA solution was applied to the cells. Electroporation was performed with an Epizap electroporation apparatus by applying a series of 4 pulses of 50 V with a capacitance of 1.0 µF. F12 growth medium was immediately added and the dishes were returned to the incubator. The cells were imaged by fluorescence microscopy 24–48 hours later.

Transfection by PolyFect Reagent

CHO-K1 or HEK293 cells were plated on MatTek dishes. For transfection, the procedure outlined in the PolyFect Transfection Reagent Handbook was followed. 1.5 µg wt-EGFP or S29TAG-EGFP DNA was diluted to a total volume of 100 µL in serum-free F12 (for CHO-K1 cells) or DMEM (for HEK293 cells). 10 µL PF was added to the solution and mixed thoroughly. The solution was incubated for 10 minutes at room temperature. The medium was removed from the cells, and 1.5 mL of fresh growth medium was reapplied. 600 µL of growth medium was then mixed into the DNA/PF solution and added to the dish. The dish was returned to the incubator. Other amounts of DNA and PF were also used in initial experiments to determine the optimal conditions. The cells were imaged by fluorescence microscopy 24–48 hours later.

MPG and Antp Delivery of tRNA

Cells were transfected by Epizap or PF with S29TAG-EGFP DNA. ~24 hours after transfection, solutions of peptide and HSAS were prepared in serum-free F12 (for CHO-K1 cells) or DMEM (for HEK293 cells) and left for ~30 minutes to allow complexation to occur. The volumes of the solutions were 20 μ L for Epizap slides and 50 μ L for MatTek dishes, and typical concentrations were 50 or 100 μ M peptide and 0.25, 0.5, or 0.8 μ M HSAS, giving charge ratios of 10/1, 5/1, or 3/1. The medium was removed from the dish, and the peptide/HSAS solutions were applied to the wells in the dishes for ~60 minutes at 37 °C. 2 mL fresh growth medium was added to the dishes and they were returned to the incubator. The cells were imaged by fluorescence microscopy 24–48 hours later.

Production of Tat-eEF1A Fusion Protein

Materials

The gene for *Xenopus laevis* eEF1A was obtained from the mMessage mMachine kit, which was purchased from Ambion (Austin, TX). Synthetic DNA oligonucleotides were synthesized by an ABI 394 DNA Synthesizer on site. The pTAT plasmid was a generous gift from Steven Dowdy (Washington University). Rosetta(DE3) cells were purchased from Novagen (San Diego, CA). Luria Broth (LB) was purchased from DIFCO. Terrific Broth (TB) was purchased from Invitrogen (Carlsbad, CA). Ready Gels, 5x TBE buffer, and 40% 29:1 acrylamide:bisacrylamide were purchased from Bio-Rad (Hercules, CA). Ni-NTA Superflow beads were purchased from Qiagen (Valencia, CA). EDTA-free protease inhibitor cocktail pellets were purchased from Roche

(Indianapolis, IN). Centricon Plus-80 concentrators were purchased from Millipore (Billerica, MA).

Mutagenesis and Plasmid Generation

Two synthetic oligonucleotide primers were designed to add a KpnI restriction site just to the 5' side of the gene and an EcoRI site just to the 3' side. PCR was used to incorporate these primers into the eEF1A gene. Using the restriction enzymes, the gene was inserted into the pTAT plasmid, which contains a T7 promoter, a sequence encoding the Tat PTD, and a polylinker allowing for easy generation of Tat-fusion proteins. The proper insertion of the gene was confirmed by DNA sequencing. The peptide sequence appended to the N-terminus of eEF1A was

MRGSHHHHHHHGMASMTGGQMGRLDYDDDDKDRWGSKLGYGRKKRRQRRR
GGSTMAGTT, where both the 6His tag and the Tat PTD are underlined. The gene encoded a 521 amino acid protein with a molecular weight of 57 kD.

Transformation and Overexpression

The pTAT plasmid containing the Tat-eEF1A gene was transformed into Rosetta(DE3) competent cells. This cell line is identical to the BL21(DE3) cell line, except it contains an additional chloramphenicol-resistant plasmid that encodes six tRNA genes with anticodons that are rare in *E. coli* but abundant in eukaryotic genes: AGG and AGA (Arg), AUA (Ile), CUA (Leu), CCC (Pro), and GGA (Gly). Therefore, it is recommended for use in overexpressing eukaryotic proteins. Because 30 of the 521 codons in the Tat-eEF1A gene (5.8%) are among these six, the Rosetta cell line provided

a significant advantage over other cell lines. The cells were plated on agar plates of LB+Amp.

A seed culture for overexpression of the protein was started by picking a colony from the plate and growing overnight in 25 mL LB+Amp. The entire seed culture was poured into 500 mL TB+Amp and incubated until the OD₆₀₀ reached 0.6–0.8. A 1 mL aliquot of the culture was removed as the uninduced control. Protein expression was induced by adding IPTG to a final concentration of 0.4 mM, and the culture was grown for 2 more hours. A 1 mL aliquot was again removed as the induced control. The cells were pelleted by centrifugation for 20 minutes at 6000g and 4 °C.

In preparation for analysis by sodium dodecyl sulfate-polyacrylamide gel electrophoresis (SDS-PAGE), the control samples were pelleted by microcentrifugation. The pellets were washed twice in 1.5 mL cold phosphate buffered saline (PBS) and resuspended in 50 µL water. 50 µL of 2x SDS loading buffer was added, and the solutions were boiled for 5 minutes.

Protein Purification from Inclusion Bodies

The protocol for the isolation of proteins from inclusion bodies was obtained from the lab of Pamela Bjorkman (Caltech), available at the link for “Inclusion body preparation” on her website (<http://www.its.caltech.edu/~bjorker/protocols.html>).

Solution buffer consisted of 50 mM Tris-Cl, 25% sucrose, 1 mM NaEDTA, 0.1% NaN₃, and 10 mM DTT, pH 8.0. Lysis buffer consisted of 50 mM Tris-Cl, 1% Triton X-100, 1% sodium deoxycholate, 100 mM NaCl, 0.1% NaN₃, and 10 mM DTT, pH 8.0. Washing buffer without Triton X-100 contained 50 mM Tris-Cl, 100 mM NaCl, 1 mM

NaEDTA, 0.1% NaN₃, and 1 mM DTT, pH 8.0. Washing buffer with Triton X-100 was also prepared by including 0.5% Triton X-100 in the above washing buffer.

The bacterial pellet was suspended in 13 mL solution buffer on ice and transferred to a 30 mL centrifugation bottle. It was probe sonicated for 2 pulses of 30 seconds each at level 75 (~12 W). 5 mg lysozyme, 125 U DNaseI, and 25 µL 500 mM MgCl₂ were added, and the mixture was vortexed. 12 mL of lysis buffer was added, and the mixture was incubated for 45 minutes at room temperature. 372 µL 500 mM NaEDTA in 50 mM Tris-Cl, pH 8.0 was added, and the mixture was rapidly frozen in liquid nitrogen, then thawed at 37 °C for 30 minutes. 100 µL 500 mM MgCl₂ was added, and the mixture was incubated for 45 minutes at room temperature. 372 µL 500 mM NaEDTA in 50 mM Tris-Cl, pH 8.0 was again added. All the remaining steps were done on ice. The mixture was pelleted by centrifugation for 20 minutes at 11,000g and 4 °C, and 1 mL of the supernatant was saved as supernatant 1. The pellet was resuspended in 10 mL wash buffer with Triton X-100 and probe sonicated as above. The mixture was again pelleted as above, and 1 mL of the supernatant was saved as supernatant 2. The pellet was resuspended in 10 mL wash buffer without Triton X-100 and probe sonicated as above. The mixture was pelleted as above, and 1 mL of the supernatant was saved as supernatant 3. The final pellet consisting of the inclusions bodies was dissolved in 9 mL of a solution of 8 M guanidinium chloride (GuCl) and 4 mM DTT by shaking at room temperature. Often, the dissolution of the pellet required more than a day of shaking.

The samples were analyzed for purity by SDS-PAGE. The uninduced and induced expression control samples, supernatants 1, 2, and 3, and the final protein sample were run on a 7.5% Tris-Cl Ready Gel at ~150 V for ~1 hour. The protein was visualized

by staining with Coomassie brilliant blue. Because the mixture of GuCl and SDS precipitates out of solution, which blocks the flow of current, the protein sample was diluted fourfold in water before loading in the gel.

Purification of Tat-eEF1A Using Ni-NTA Beads

~5 µg denatured Tat-eEF1A, dissolved in 8 M GuCl and 4 mM DTT, was incubated with 1–2 mL of Ni-NTA Superflow beads for ~2 hours while shaking at room temperature. The beads have a binding capacity of 5–10 mg protein/mL. The mixture was poured into a small fritted column. The flowthrough was reapplied to the beads in the column several times, and the final flowthrough was collected. The beads were washed with 8 mL of 6 M GuCl, pH 6.3, and the wash solution was also collected. The protein was eluted from the beads by four applications of 1 mL of 6 M GuCl, pH 4.5. Each mL of the eluted solution was saved.

Refolding and Binding Assay

Refolding of the Tat-eEF1A (with or without the Ni-NTA purification) was attempted in eight buffers, which contained all possible combinations of 0 or 400 mM arginine (Arg), 0 or 500 mM GuCl, and 0 or 20% glycerol. Also, each buffer contained 50 mM Tris-Cl, 20 mM NaCl, 10 mM MgCl₂, 10 mM DTT and 1 pellet of EDTA-free protease inhibitor cocktail. The pH was brought to 6.8. 1–2 mg of protein in 8 M GuCl solution was slowly dripped into 80 mL of the various refolding buffers, and gently stirred for ~8 hours. The solutions were then passed through a 0.2 µm filter and concentrated using Centricon Plus-80 concentrators, reducing the volume to 1 mL or less.

Protein content in the filtrates and retentates was analyzed by SDS-PAGE, as described above.

To activate the eEF1A with GTP before tRNA complexation, EF buffer was prepared as in [54]: 40 mM HEPES, 100 mM NH₄Cl, 10 mM MgCl₂, 1 mM DTT, pH 7.5. 4x loading buffer for native PAGE consisted of 1% bromophenol blue and 60% glycerol. 10 μ L solutions were prepared from 2 μ L 5x EF buffer, 3.5 μ L 4x loading buffer, 1 μ L 30 mM GTP, ~4 or ~1 μ g Tat-eEF1A (~70 or ~15 pmol), and 0.25 μ g HSAS (10 pmol). Before HSAS addition, all components (except HSAS) were incubated at 30 °C for 20 minutes to activate eEF1A with GTP. The samples were then run on a native PAGE gel.

Native PAGE gels were prepared in the following manner. A solution of 1x TBE pH 8.3, 12.5% glycerol, and 10% acrylamide (29:1 acrylamide:bisacrylamide), and a separate solution of 10% ammonium persulfate were prepared. Both solutions and TEMED were kept on ice. When sufficiently cold, 112 μ L ammonium persulfate solution and 5 μ L TEMED were added to 7.5 mL of TBE solution. The mixture was shaken and immediately poured into the gel caster. It was allowed to polymerize for several hours. The gel composition was similar to that used previously for a gel-shift assay for tRNA/synthetase binding [60], although the amounts of Tris, boric acid, and EDTA were not identical because we used a Bio-Rad premixed buffer, and the glycerol amount was increased slightly. For horizontal gels in the casters that are normally used for agarose gels, the solution amounts were scaled up 2.5-fold. The protein and tRNA were visualized by silver staining.

REFERENCES

1. Berg, J. M., J. L. Tymoczko, and L. Stryer. 2002. *Biochemistry, Fifth Edition*. New York: W. H. Freeman and Company.
2. Fersht, A. 1999. *Structure and Mechanism in Protein Science*. New York: W. H. Freeman and Company.
3. England, P. M. 2004. Unnatural amino acid mutagenesis: A precise tool for probing protein structure and function. *Biochemistry*. 43:11623-11629.
4. Cashin, A. L., E. J. Petersson, H. A. Lester, and D. A. Dougherty. 2005. Using physical chemistry to differentiate nicotinic from cholinergic agonists at the nicotinic acetylcholine receptor. *J. Am. Chem. Soc.* 127:350-356.
5. England, P. M., H. A. Lester, N. Davidson, and D. A. Dougherty. 1997. Site-specific, photochemical proteolysis applied to ion channels *in vivo*. *Proc. Natl. Acad. Sci. USA*. 94:11025-11030.
6. Gallivan, J. P., H. A. Lester, and D. A. Dougherty. 1997. Site-specific incorporation of biotinylated amino acids to identify surface-exposed residues in integral membrane proteins. *Chem. Biol.* 4:739-749.
7. Petersson, E. J., G. S. Brandt, N. M. Zacharias, D. A. Dougherty, and H. A. Lester. 2003. Caging proteins through unnatural amino acid mutagenesis. *Methods Enzymol.* 360:258-273.
8. Zhong, W., J. P. Gallivan, Y. Zhang, L. Li, H. A. Lester, and D. A. Dougherty. 1998. From *ab initio* quantum mechanics to molecular neurobiology: A cation- π binding site in the nicotinic receptor. *Proc. Natl. Acad. Sci. USA*. 95:12088-12093.
9. Ellman, J., D. Mendel, S. Anthony-Cahill, C. J. Noren, and P. G. Schultz. 1991. Biosynthetic method for introducing unnatural amino acids site-specifically into proteins. *Methods Enzymol.* 202:301-336.
10. Noren, C. J., S. J. Anthony-Cahill, M. C. Griffith, and P. G. Schultz. 1989. A general method for site-specific incorporation of unnatural amino acids into proteins. *Science*. 244:182-188.
11. Nowak, M. W., J. P. Gallivan, S. K. Silverman, C. G. Labarca, D. A. Dougherty, and H. A. Lester. 1998. *In vivo* incorporation of unnatural amino acids into ion channels in *Xenopus* oocyte expression system. *Methods Enzymol.* 293:504-529.
12. Nowak, M. W., P. C. Kearney, J. R. Sampson, M. E. Saks, C. G. Labarca, S. K. Silverman, W. Zhong, J. Thorson, J. N. Abelson, N. Davidson, P. G. Schultz, D. A. Dougherty, and H. A. Lester. 1995. Nicotinic receptor binding site probed with unnatural amino acid incorporation in intact cells. *Science*. 268:439-442.

13. Monahan, S. L., H. A. Lester, and D. A. Dougherty. 2003. Site-specific incorporation of unnatural amino acids into receptors expressed in mammalian cells. *Chem. Biol.* 10:573-580.
14. Bogoyevitch, M. A., T. S. Kendrick, D. C. Ng, and R. K. Barr. 2002. Taking the cell by stealth or storm? Protein transduction domains (PTDs) as versatile vectors for delivery. *DNA Cell Biol.* 21:879-894.
15. Deshayes, S., M. C. Morris, G. Divita, and F. Heitz. 2005. Cell-penetrating peptides: Tools for intracellular delivery of therapeutics. *Cell. Mol. Life Sci.* 62:1839-1849.
16. Fischer, P. M., E. Krausz, and D. P. Lane. 2001. Cellular delivery of impermeable effector molecules in the form of conjugates with peptides capable of mediating membrane translocation. *Bioconjug. Chem.* 12:825-841.
17. Fischer, R., M. Fotin-Mleczek, H. Hufnagel, and R. Brock. 2005. Break on through to the other side—biophysics and cell biology shed light on cell-penetrating peptides. *Chembiochem.* 6:2126-2142.
18. Derossi, D., A. H. Joliot, G. Chassaing, and A. Prochiantz. 1994. The third helix of the Antennapedia homeodomain translocates through biological membranes. *J. Biol. Chem.* 269:10444-10450.
19. Vives, E., P. Brodin, and B. Lebleu. 1997. A truncated HIV-1 Tat protein basic domain rapidly translocates through the plasma membrane and accumulates in the cell nucleus. *J. Biol. Chem.* 272:16010-16017.
20. Bonny, C., A. Oberson, S. Negri, C. Sauser, and D. F. Schorderet. 2001. Cell-permeable peptide inhibitors of JNK: Novel blockers of beta-cell death. *Diabetes.* 50:77-82.
21. Fujimoto, K., R. Hosotani, Y. Miyamoto, R. Doi, T. Koshiba, A. Otaka, N. Fujii, R. D. Beauchamp, and M. Imamura. 2000. Inhibition of pRb phosphorylation and cell cycle progression by an antennapedia-p16(INK4A) fusion peptide in pancreatic cancer cells. *Cancer Lett.* 159:151-158.
22. Rousselle, C., P. Clair, J. M. Lefauconnier, M. Kaczorek, J. M. Scherrmann, and J. Temsamani. 2000. New advances in the transport of doxorubicin through the blood-brain barrier by a peptide vector-mediated strategy. *Mol. Pharmacol.* 57:679-686.
23. Waizenegger, T., R. Fischer, and R. Brock. 2002. Intracellular concentration measurements in adherent cells: a comparison of import efficiencies of cell-permeable peptides. *Biol. Chem.* 383:291-299.
24. Sahai, E., M. F. Olson, and C. J. Marshall. 2001. Cross-talk between Ras and Rho signalling pathways in transformation favours proliferation and increased motility. *EMBO J.* 20:755-766.

25. Schwarze, S. R., A. Ho, A. Vocero-Akbani, and S. F. Dowdy. 1999. *In vivo* protein transduction: Delivery of a biologically active protein into the mouse. *Science*. 285:1569-1572.
26. Soga, N., N. Namba, S. McAllister, L. Cornelius, S. L. Teitelbaum, S. F. Dowdy, J. Kawamura, and K. A. Hruska. 2001. Rho family GTPases regulate VEGF-stimulated endothelial cell motility. *Exp. Cell Res.* 269:73-87.
27. Allinquant, B., P. Hantraye, P. Mailleux, K. Moya, C. Bouillot, and A. Prochiantz. 1995. Downregulation of amyloid precursor protein inhibits neurite outgrowth in vitro. *J. Cell. Biol.* 128:919-927.
28. Troy, C. M., D. Derossi, A. Prochiantz, L. A. Greene, and M. L. Shelanski. 1996. Downregulation of Cu/Zn superoxide dismutase leads to cell death via the nitric oxide-peroxynitrite pathway. *J. Neurosci.* 16:253-261.
29. Villa, R., M. Folini, S. Lualdi, S. Veronese, M. G. Daidone, and N. Zaffaroni. 2000. Inhibition of telomerase activity by a cell-penetrating peptide nucleic acid construct in human melanoma cells. *FEBS Lett.* 473:241-248.
30. Lewin, M., N. Carlesso, C. H. Tung, X. W. Tang, D. Cory, D. T. Scadden, and R. Weissleder. 2000. Tat peptide-derivatized magnetic nanoparticles allow *in vivo* tracking and recovery of progenitor cells. *Nat. Biotechnol.* 18:410-414.
31. Torchilin, V. P., R. Rammohan, V. Weissig, and T. S. Levchenko. 2001. TAT peptide on the surface of liposomes affords their efficient intracellular delivery even at low temperature and in the presence of metabolic inhibitors. *Proc. Natl. Acad. Sci. USA.* 98:8786-8791.
32. Kramer, S. D., and H. Wunderli-Allenspach. 2003. No entry for TAT(44-57) into liposomes and intact MDCK cells: Novel approach to study membrane permeation of cell-penetrating peptides. *Biochim. Biophys. Acta.* 1609:161-169.
33. Leifert, J. A., S. Harkins, and J. L. Whitton. 2002. Full-length proteins attached to the HIV tat protein transduction domain are neither transduced between cells, nor exhibit enhanced immunogenicity. *Gene Ther.* 9:1422-1428.
34. Leifert, J. A., and J. L. Whitton. 2003. "Translocatory proteins" and "protein transduction domains": A critical analysis of their biological effects and the underlying mechanisms. *Mol. Ther.* 8:13-20.
35. Richard, J. P., K. Melikov, E. Vives, C. Ramos, B. Verbeure, M. J. Gait, L. V. Chernomordik, and B. Lebleu. 2003. Cell-penetrating peptides. A reevaluation of the mechanism of cellular uptake. *J. Biol. Chem.* 278:585-590.
36. Thoren, P. E., D. Persson, P. Isakson, M. Goksor, A. Onfelt, and B. Norden. 2003. Uptake of analogs of penetratin, Tat(48-60) and oligoarginine in live cells. *Biochem. Biophys. Res. Commun.* 307:100-107.

37. Terrone, D., S. L. Sang, L. Roudaia, and J. R. Silvius. 2003. Penetratin and related cell-penetrating cationic peptides can translocate across lipid bilayers in the presence of a transbilayer potential. *Biochemistry*. 42:13787-13799.
38. Thoren, P. E., D. Persson, M. Karlsson, and B. Norden. 2000. The antennapedia peptide penetratin translocates across lipid bilayers—the first direct observation. *FEBS Lett.* 482:265-268.
39. Tung, C. H., and S. Stein. 2000. Preparation and applications of peptide-oligonucleotide conjugates. *Bioconjug. Chem.* 11:605-618.
40. Derossi, D., G. Chassaing, and A. Prochiantz. 1998. Trojan peptides: The penetratin system for intracellular delivery. *Trends Cell Biol.* 8:84-87.
41. Igloi, G. L. 1988. Interaction of tRNAs and of phosphorothioate-substituted nucleic acids with an organomercurial. Probing the chemical environment of thiolated residues by affinity electrophoresis. *Biochemistry*. 27:3842-3849.
42. Monahan, S. L. 2004. Site-specific incorporation of unnatural amino acids into receptors expressed in mammalian cells. Ph.D. thesis, California Institute of Technology.
43. Karim, A. S., C. S. Johansson, and J. K. Weltman. 1995. Maleimide-mediated protein conjugates of a nucleoside triphosphate gamma-S and an internucleotide phosphorothioate diester. *Nucleic Acids Res.* 23:2037-2040.
44. Karim, A. S., and J. K. Weltman. 1993. Formation of protein conjugates of phosphorothioate nucleoside diphosphate beta-S. *Nucleic Acids Res.* 21:5281-5282.
45. Madhusoodanan, K. S., and R. F. Colman. 2001. Adenosine 5'-0-[S-(4-succinimidyl-benzophenone)thiophosphate]: a new photoaffinity label of the allosteric ADP site of bovine liver glutamate dehydrogenase. *Biochemistry*. 40:1577-1586.
46. Vidal, P., M. C. Morris, L. Chaloin, F. Heitz, and G. Divita. 1997. New strategy for RNA vectorization in mammalian cells. Use of a peptide vector. *C. R. Acad. Sci. III.* 320:279-287.
47. Morris, M. C., L. Chaloin, J. Mery, F. Heitz, and G. Divita. 1999. A novel potent strategy for gene delivery using a single peptide vector as a carrier. *Nucleic Acids Res.* 27:3510-3517.
48. Morris, M. C., P. Vidal, L. Chaloin, F. Heitz, and G. Divita. 1997. A new peptide vector for efficient delivery of oligonucleotides into mammalian cells. *Nucleic Acids Res.* 25:2730-2736.

49. Marthinet, E., G. Divita, J. Bernaud, D. Rigal, and L. G. Baggetto. 2000. Modulation of the typical multidrug resistance phenotype by targeting the MED-1 region of human MDR1 promoter. *Gene Ther.* 7:1224-1233.
50. Capone, J. P., P. A. Sharp, and U. L. RajBhandary. 1985. Amber, ochre and opal suppressor tRNA genes derived from a human serine tRNA gene. *EMBO J.* 4:213-221.
51. Pooga, M., C. Kut, M. Kihlmark, M. Hallbrink, S. Fernaeus, R. Raid, T. Land, E. Hallberg, T. Bartfai, and U. Langel. 2001. Cellular translocation of proteins by transportan. *FASEB J.* 15:1451-1453.
52. Andersen, G. R., P. Nissen, and J. Nyborg. 2003. Elongation factors in protein biosynthesis. *Trends Biochem. Sci.* 28:434-441.
53. Negrutskii, B. S., and A. V. El'skaya. 1998. Eukaryotic translation elongation factor 1 alpha: structure, expression, functions, and possible role in aminoacyl-tRNA channeling. *Prog. Nucleic Acid Res. Mol. Biol.* 60:47-78.
54. Dreher, T. W., O. C. Uhlenbeck, and K. S. Browning. 1999. Quantitative assessment of EF-1alpha. GTP binding to aminoacyl-tRNAs, aminoacyl-viral RNA, and tRNA shows close correspondence to the RNA binding properties of EF-Tu. *J. Biol. Chem.* 274:666-672.
55. Asahara, H., and O. C. Uhlenbeck. 2002. The tRNA specificity of *Thermus thermophilus* EF-Tu. *Proc. Natl. Acad. Sci. USA.* 99:3499-3504.
56. LaRiviere, F. J., A. D. Wolfson, and O. C. Uhlenbeck. 2001. Uniform binding of aminoacyl-tRNAs to elongation factor Tu by thermodynamic compensation. *Science.* 294:165-168.
57. Becker-Hapak, M., S. S. McAllister, and S. F. Dowdy. 2001. TAT-mediated protein transduction into mammalian cells. *Methods.* 24:247-256.
58. Arcari, P., M. Masullo, A. Arcucci, G. Ianniciello, B. de Paola, and V. Bocchini. 1999. A chimeric elongation factor containing the putative guanine nucleotide binding domain of archaeal EF-1 alpha and the M and C domains of eubacterial EF-Tu. *Biochemistry.* 38:12288-12295.
59. Cilly, C. D., and J. R. Williamson. 1997. Analysis of bacteriophage N protein and peptide binding to boxB RNA using polyacrylamide gel coelectrophoresis (PACE). *RNA.* 3:57-67.
60. Rubelj, I., I. Weygand-Durasevic, and Z. Kucan. 1990. Evidence for two types of complexes formed by yeast tyrosyl-tRNA synthetase with cognate and non-cognate tRNA. Effect of ribonucleoside triphosphates. *Eur. J. Biochem.* 193:783-788.